Trends in Food Science & Technology 163 (2025) 105135

Contents lists available at ScienceDirect

Trends in Food Science & Technology

journal homepage: www.elsevier.com/locate/tifs

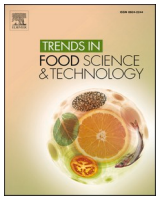

Synergic removal of Aflatoxin B1 in oily matrices by focusing on the peroxidase-like nanozymes-driven strategies: Mechanisms and intermediate toxicity, nutritional impact, advances and challenges

A.R. Faraji [a,b,*], A. Gil [c,**], A. Farahanipour [a], E. Tehrani [d], N.B. Khoramdareh [b], E. Dashtabadi [d], S. Jafari [e], N. Shojaei [d], Z. Hekmatian [f], S. Saeedi [b]

[a] Department of Organic Chemistry, TeMS.C., Islamic Azad University, Tehran, Iran
[b] Nutrition and Food Sciences Research Center, TeMS.C., Islamic Azad University, Tehran, Iran
[c] INAMAT˜2-Science Department, Los Acebos Building, Public University of Navarra, Campus of Arrosadia, E-31006, Pamplona, Spain
[d] Department of Pharmaceutical Chemistry, TeMS.C., Islamic Azad University, Tehran, Iran
[e] Department of Nano Chemistry, TeMS.C., Islamic Azad University, Tehran, Iran
[f] Department of Chemistry, Faculty of Science, Payam Noor University, Hamedan, Iran

ARTICLE INFO

Handling Editor: Dr I Oey

Keywords:
Aflatoxin B1
Nanozyme
Peroxidase-like
Enzyme-mimetic degradation
Edible oil
Detoxification

ABSTRACT

Background: Oilseeds and extracted oils, as the supplier of at least 40 % of calories, dietary essential fatty acids, and food flavor, due to insufficient cultivation-harvesting techniques, processing and long-term storage in improper conditions, and lack of adequate food-safety standards and/or official consideration, are prone to contamination by AFB1. Given its irreversible adverse effects on consumer health and food/feed safety due to various factors (*e.g.,* high chemical stability of lipophilic AFB1, transformation to other toxic derivatives, and chemical interaction with oily matrices), developing a decontamination approach from a safety/efficiency perspective is imperative.

Scope and approach: This review provides the recent progress on the AFB1 detoxification from oily matrices by focusing on the peroxidase-based nanozymes technologies and enzymatic-like mechanisms of reactive species in detail for the first time. Significantly, the superiority of enzymatic-like activity in capturing/detoxifying AFB1 from oily matrices, change in nutritional quality, organoleptic profiles, and physicochemical properties of oils, and mechanism of action are highlighted by a comparison with various edible oil remediation systems (*i.e.,* physicochemical, physical, chemical, and biological).

Key findings and conclusions: The peroxidase nanozyme–based technologies could be of primary importance in the remediation of AFB1 from oily matrices due to the unique merits of nanozymes (*e.g.,* low-cost, size/surface-dependent properties, excellent efficiency and durability/stability, recoverability, biocompatibility, many capabilities to maintain the nutritional quality, and without require to any pre-treatment). Finally, this review aimed to provide several beneficial insights regarding safety, universality, finance, ecology, rapidity, selectivity, detoxification path, and toxicity/biological nature of transformed products in peroxidase-mimicking nanozyme technologies.

1. Introduction

Mycotoxins (>500 types) are fungal-synthesized secondary metabolites with low molecular weight (<1000 Da), highly toxic, and widely distributed worldwide, which squandered the 1.3 billion metric tons of global nourishment products annually across the food supply chain (Khan et al., 2024; Song et al., 2024). The specific sort, concentration, length of exposure to mycotoxins, and age of the individual mainly influence acute toxicity and chronic illness and trigger deadly outbreaks.

Among all mycotoxins, AFB1 and its metabolites are considered the most hazardous compounds, severely impacting human/animal health (Li, Liu, et al., 2022). AFB1, generated by various toxigenic *Aspergillus*

* Corresponding author. Department of Organic Chemistry, TeMS.C., Islamic Azad University, Tehran, Iran.
** Corresponding author.
E-mail addresses: alireza_ch57@yahoo.com (A.R. Faraji), andoni@unavarra.es (A. Gil).

https://doi.org/10.1016/j.tifs.2025.105135
Received 7 February 2025; Received in revised form 18 May 2025; Accepted 7 June 2025
Available online 13 June 2025

strains, causes carcinogenic effects on organs such as the liver, heart, kidneys, lungs, intestine, and skin (Wu et al., 2021). Due to their intensified sensitivity to immunological, endocrine, nervous, and neurotoxic effects, children typically show more severe disturbances and are undefended to these toxic effects than adults. It has also been revealed that AFB1 may be transferred across the placenta from mother to fetus, potentially leading to abnormalities in infants (Javanmardi et al., 2022; Li, Liu, et al., 2022). According to reports in the literature, AFB1 contamination has led to high annual rates of liver cancer (>1.50 $\times$ 10^5 cases), which is more prevalent in *Southeast Asia* and *South Africa* and leads to the second most prevalent type of cancer in China (Guo et al., 2021; Liu & Wu, 2010). Therefore, the WHO (*World Health Organization*) and IARC (*International Agency for Research on Cancer*) have classified AFB1 as a first-grade carcinogen that affects the nutritional quality of food/feed, production performance, global ecosystem, and public health.

Large numbers of agricultural products (*e.g.,* oil seeds and their derived product) and foods under unsuitable processing/storage conditions are susceptible to contamination with AFB1. It should be noted that lipophilic-AFB1 metabolites remain stable in oily food matrices during the production/refining processes (*i.e.,* degumming, neutralization, bleaching, and deodorization) while may deactivating certain compounds (*i.e.,* enzymes, antioxidants, and vitamins) (Zhou et al., 2024; Abraham et al., 2023). The *Food and Drug Administration* and *European Commission* have established that the acceptable limits for AFB1 in foodstuffs intended for human consumption are between 2.0 μg kg^{-1} and 20.0 μg kg^{-1}, respectively (Ji & Xie, 2021; Song et al., 2024). Additionally, 20.0 μg kg^{-1} AFB1 in maize, peanut, and corn oils and 10.0 μg kg^{-1} AFB1 in other edible oils have been set as the maximum permissible limit in China. Long-term and/or improper storage causes contamination of oil products by AFB1 at high levels; thus, many countries have set the lowest threshold value for aflatoxins in products and products (Fig. 1) (Bordin et al., 2014; Cavaliere, 2007; Chen et al., 2019; Deng et al., 2018; Einolghozati et al., 2021; Javanmardi et al., 2022; KAMIMURA et al., 1986; Karunarathna et al., 2019; Mohammed et al., 2018; Pitta & Markaki, 2010; Yang et al., 2011; Zhang & Xu, 2019; Zhao et al., 2017). Therefore, significant progress in the deterioration process (in design, fabrication, characterization, functionalization,

Fig. 1. The prevalence of AFB1 in edible oils. [P/N (%): Amount of pollution; R: Range; SD: Standard deviation; M: Analysis method; LOD: Limit of detection; PL: Permitted level].

implementation, and efficiency) has become a fundamental attitude for researchers regarding food safety/quality (Nazhand et al., 2020).

A wide range of methods, such as physical (*e.g.,* several irradiations, photocatalysts), chemical (*e.g.,* ozonation, oxidizing agents, and electrolyzed oxidizing water), biological (*e.g.,* microorganisms and enzymes), and physicochemical based on absorption have been used for the AFB1 detoxification from oily food matrices (Rushing & Selim, 2019). Biological methods are rarely utilized in the large-scale industrial decontamination of AFB1 due to stringent operational conditions and the complexities associated with its metabolites. In contrast, physical and chemical methods are more feasible for detoxifying AFB1 from oils. However, chemical methods often result in solvent residues, leading to secondary pollution and adversely affecting the oil's nutritional quality. Since oil matrices are lipophilic, they can retain non-polar organic solvents (*e.g.,* hexane, chloroform, and acetone) and polar solvents (*e.g.,* methanol and ethanol). On the other hand, complete removal of these solvents requires intense heating, which can lead to the degradation of the oil structure or the formation of undesirable compounds such as oxidized fatty acids. This process is highly costly and time-consuming on an industrial scale. As a result, significant solvent residues can be detected in the final product, which may impart unpleasant flavors and odors, primarily when solvents like chloroform and acetone have been used (Hron Sr et al., 1994; Cole and Dorner, 1994; Rayner, Koltun, and Dollear, 1977). Additionally, as excessive radiation can negatively impact oil quality, it is essential to regulate the duration/intensity of radiation as part of the challenges of the physical detoxification process (Ma et al., 2021; Zhang et al., 2022). Thus, to maintain high AFB1 removal performance without loss of nutritional quality of oily samples, hybrid material on a nanoscale with unique physiochemical properties has become a key (Faraji et al., 2024; Robert & Meunier, 2022).

Nanozyme-based technologies have piqued the curiosity of researchers owing to the superior AFB1 degradation efficiency via synergism between artificial enzymes and engineered nanoparticle properties (Faraji et al., 2023; Wang et al., 2025; Wei et al., 2022; Zabeti et al., 2024; Zhou et al., 2024). Among the diverse classes of nanozymes (based on metal oxide, mono-, bi- and tri-metallic, biochar, and hybrids), the peroxidase/oxidase-like nanozymes have gained significant attention as adequate substitutes for natural enzymes in detoxifying foodborne toxins (Robert & Meunier, 2022; Wang et al., 2025). Specifically, the AFB1 degradation by nanomaterial-based composites with properties similar to enzymes in redox reactions offers several outstanding merits, including facile and scale-up production, high surface-area-to-volume ratio, cost-effectiveness, non-toxicity, biocompatibility, and exceptional stability/durability under extreme environmental conditions (*e.g.,* fluctuations in pH/temperature and chemical agent interference) (Faraji et al., 2023; Zabeti et al., 2024). Furthermore, excellent AFB1 degradation by peroxidase-like nanozyme, attributed to the large surface area and tailored nanostructures, preserves the physicochemical/nutritional properties and micronutrient content of food, combined with their environmentally benign nature, and no challenges in acquisition/preservation compared to natural enzymes, making them a focal point of contemporary research in food safety and detoxification technologies (Demkiv et al., 2021; Jiang et al., 2019). Therefore, with the rapid evolution of nanotechnology, many nanomaterial-based composites provide tremendous opportunities for synergistic reduction of the level of AFB1 in oily samples.

To the best of our knowledge, this is the first comprehensive review on peroxidase-like based nanozyme in detoxification of AFB1 from edible oils. Thus, to highlight the significance of nanozymes in food processing treatments, this review scrutinizes research efforts on various peroxidase-nanozymes from oily food matrices for the first time, especially emphasizing catalytic mechanisms, electron-transfer pathways, and nutritional value changes. Then, the latest detailed information about all the reported AFB1 detoxification methods (*i.e.,* physicochemical, physical, chemical, biological, hybrid) from oily matrices has been elaborated and compared in terms of safety, capacity, universality, finance, ecology, effectivity, rapidity, selectivity, quality/organoleptic/nutritional changes, and mechanism of action with peroxidase mimicking nanozyme for the first time. Additionally, this literature review summarizes all the updated properties of the AFB1 in terms of potential toxicity in animals/humans, mechanism of action, pathogenicity and occurrence of adverse effects, and variations of AFB1 prevalence in oily matrices in the different regions. Additionally, the comprehensive comparison of an enzyme-mimetic degradation mechanism with all reported paths and the expression of transformed species' toxicity/biological nature is another distinctive feature of this review. Finally, the challenges and prospects that need to be addressed to facilitate the remediation strategies of mycotoxins from oily food matrices are also evaluated.

2. Updated information on the toxicity effect of AFB1

AFB1 is found in agricultural commodities, foodstuffs, and human/animal urine and feces, released into the sewage and surface water and reused by plants to create a contaminated closed-loop system (Rushing & Selim, 2019; Zhang et al., 2022). Carcinogenic AFB1 is transmitted to the human body through dermal absorption, intake of contaminated food/feed from vegetal/animal origin, and inhalation of fecal-contaminated dust particles. With the help of the passive diffusion mechanism, >80 % of AFB1 entered through dietary intake is absorbed in the primary and middle parts of the small intestine (Li, Liu, et al., 2022; Nazareth et al., 2024). Hazardous/unpleasant impacts of AFB1 have been found in the *hepatic*, *kidney*, *respiratory tract*, *reproductive organs*, *digestive*, *neurological*, and *immunological* systems (Li, Liu, et al., 2022). Indeed, chronic dietary exposure to AFB1 has been related to a high incidence of hepatic cancer, impaired blood-testis barrier, child growth retardation, and leukemia. Furthermore, AFB1 contributes to stunting and malnutrition diseases, such as *kwashiorkor*, *marasmic-kwashiorkor* (*marasmus*), and *gastro-enteritis*, possibly by interfering with the absorption of vital micronutrients (such as Cu, Fe, Zn, vitamins, *etc.*), metabolic enzyme activities, and protein synthesis (Francis et al., 2024). As well as, Long-term exposure to AFB1 can lead to acute aflatoxicosis, evincing drastic disease, oxidative stress, and death due to harm to the heart, kidneys, liver, reproductive organs (premature birth or miscarriage), and other organs (Guo et al., 2021; Marchese et al., 2018).

The presence of *coumarin* moiety in the structure of AFB1 causes toxicity in different organs and carcinogenic activities after the metabolic conversion of the terminal *alkene* bond of the furan ring to the epoxide, which is a much more toxic species than AFB1 (Song et al., 2024; Sun, He, et al., 2023). AFB1 can disrupt cell function, disturb the balance of the activities of cellular organelles, and induce cancer cells via bonding with guanine in DNA (*aflatoxin-N_7–guanine*), an organic base insoluble in water (Bukowska et al., 2024; Dai et al., 2024). In addition to the aforementioned adverse effects, recent studies have shown that the presence of AFB1 in oil-based matrices increases its stability and enhances its bioavailability and toxicity (Lin et al., 2019). According to a study conducted by Jubeen et al. (2022), it was inferred that among 100 edible oil samples, including canola, soybean, and sunflower oils, approximately 89.0 % were contaminated with AFB1. Notably, 65 % of these samples contained levels exceeding the EU's permissible limit of 20.0 μg kg^{-1}, with canola oil exhibiting the highest contamination. Specifically, in 71.0 % of canola oil samples, AFB1 concentrations ranged from 54.4 to 281.1 μg kg^{-1}. On the other hand, common thermal cooking processes like frying cannot eliminate them, threatening consumer health. Finally, a quantitative assessment of liver cancer risk due to the consumption of these oils was conducted using models such as the Margin of Exposure and Quantitative Risk Assessment. The findings indicated that long-term consumption of contaminated oils, especially canola oil, significantly increases the risk of developing hepatocellular carcinoma. For instance, the estimated incidence rate was 17.13 cases per 100,000 individuals in men over 35 years

of age and 10.93 cases in women (Jubeen et al., 2022).

The lethal dose (LD_{50}) value for AFB1 varies depending on the animal species, age, and route of administration (oral, injectable, etc.). While the average LD_{50} in rats via intraperitoneal injection has been reported to be ~0.36 mg kg^{-1}, the LD_{50} range for oral administration across different animal species varies from 1.0 to 50.0 mg kg^{-1}. The intraperitoneal injection produces higher toxicity than oral administration (Hanigan & Laishes, 1984; Panel et al., 2020). Also, it demonstrates highly toxic effects, with an LD_{50} of less than 1.0 mg kg^{-1} in particular species, including cats, dogs, ducklings, rainbow trout, and pigs (Bilgrami & Sinha, 2024; Rawal et al., 2010). Besides, AFB1 increases inflammatory effects, destroys hepatic and gut tissues, and reduces the function of white blood cells such as thymocytes and lymphocytes, ultimately leading to cell death. All the mentioned factors will inevitably decrease the efficiency of animals in the long run, particularly in the livestock and poultry production sectors, which will finally lead to colossal financial damages (Li, Liu, et al., 2022; Saha et al., 2024). In another study, rats were orally administered AFB1 dissolved in olive oil, and the results showed that such exposure led to increased oxidative stress and alterations in hepatic mitochondrial lipids. Moreover, elevated levels of liver enzymes (ALT, AST) and histopathological damage were observed (Rotimi et al., 2019).

3. AFB1 decontamination techniques for oily matrices

3.1. Physical methods

The physical techniques (*i.e.,* heat application, cooking, roasting, irradiations, and photocatalyst) for AFB1 decontamination can be categorized into extraction and degradation technology (Guo et al., 2021). Liu et al. (2011) indicated that both the intensity of UV light (200–800 μw cm^{-2}) and the duration of irradiation were critical factors influencing the AFB1 photodegradation from peanut oils. Additionally, the *mammalian erythrocyte micronucleus* assay validated the safety of the detoxified edible oils, as the mutagenic activity present in untreated control oil was eliminated in the UV-treated samples. Also, Wang et al. (2020) utilized ultraviolet light-emitting diodes (UV-LED) to assess the quality of AFB1-detoxified unrefined groundnut oils. 20-minute treatment resulted in a 99.0 % reduction of AFB1 content. The heat produced by LED technology is significantly lower than that generated by conventional UV lamps, making it a more appropriate choice for food treatment applications and more energy-efficient. Compared to UV, gamma rays exhibit superior penetration capabilities in liquid/solid materials, enabling them to eliminate AFB1 by generating reactive species from H_2O/coexisting constituents. There was no considerable impact on the nutritional value, amount of tocopherol, or oxidative stability of gamma-treated soybean oil samples (<20.0 kGy) over 30 days (Zhang et al., 2018). Besides, TiO_2 is a promising method for AFB1 photodecontamination, attributed to its robust redox capabilities, eco-friendliness, stability, sustainable treatment options, and cost-effectiveness. When light rays are directed onto TiO_2, the generated h^+/e^- can interact with H_2O/O_2, leading to the formation of $O_2^{\bullet-}$ and $^{\bullet}OH$ for the attack on AFB1 molecules (Magzoub et al., 2019). The magnetic graphene oxide/TiO_2 (MGO/TiO_2) composite with extensive surface area and superior conductivity exhibited effective performance (96.40 %) in reducing AFB1 levels in corn oil through a straightforward photocatalytic process under both UV and visible light conditions without nutrient losses (Sun et al., 2020). The proposed mechanism involves key active species, including h^+ and $^{\bullet}OH$, which can target the reactive sites of AFB1. Furthermore, the Ag-phosphotungstate/polyimide, I_2-doped on the TiO_2 thin film, and porous graphitic carbon nitride/graphene oxide hydrogel microsphere are introduced as an effective system for reducing AFB1 levels in oily matrices (see Table 1). In addition, the operational parameters (*e.g.,* intensity, wavelength, irradiation time, temperature, pH, and the type of oil matrix) affecting AFB1 removal rates and provides new directions for optimizing them to increase detoxification efficiency. The removal rate is typically enhanced with increasing intensity, irradiation time, and temperature. Above optimal conditions, there is no significant increase in efficiency; in some cases, it leads to changes in food quality. For example, increasing the irradiation dose from 300 to 1200 mJ cm^{-2} at a wavelength of 365 nm resulted in an AFB1 removal efficiency of 96.0 % after 30 min (Mao et al., 2016). Additionally, most studies employing the mentioned methods have been conducted under ambient conditions, *i.e.,* room temperature (25–30 °C) and neutral pH (6.0–7.0). However, changes in catalyst surface behavior, alterations in reaction rates, and compound stability contribute to a decrease in detoxification efficiency under highly acidic or alkaline pH values and temperatures outside the room temperature range. In the TiO_2-based photocatalysts, the removal efficiency of AFB1 decreased by 30.0–60.0 % under acidic conditions (pH = ~3.0). In contrast, near-neutral pH and room temperature conditions led to an efficiency exceeding 99.0 % (Magzoub et al., 2019). Additionally, in another study using the pulsed light process, irradiation-induced temperature increases up to 220 °C led to a removal efficiency of 78.2 % for AFB1. However, this also negatively impacted the oil's quality indices, such as AV, PV, and FFAs. According to existing studies, the type of oil matrix (*e.g.,* fat content, polarity, acidity, and impurities) can significantly affect the performance of physical methods for AFB1 removal (Javanmardi et al., 2022).

3.2. Chemical methods

Chemical approaches involve the decomposition of AFB1 molecular structure by applying various chemical substances (Pankaj et al., 2018). Alkaline solutions such as NaOH and KOH play a dual role in alkaline refining, removing free fatty acids and effectively reducing AFB1 levels in oily matrices. The AFB1 concentration declined from 34.78 to 0.370 μg kg^{-1} at a temperature of 43.50 °C using a 23.40 % NaOH solution (Table 1). Interestingly, an increase in temperature to 77.1 °C had no significant effect on the removal efficiency, likely due to the thermal stability of AFB1. In addition, *Ames* tests and *$HepG_2$* cell viability assessments demonstrated that alkali treatment enhances the safety of treated oils (Ji et al., 2016). Conversely, Yassin and Abdelrahman (2019) revealed that alkaline refining had minimal impact on the AFB1 degradation from peanut oil. The improvement in oil quality was attributed solely to reductions in AV, FFA, and MC. Following approval by the FDA in recent years, O_3, as a highly reactive/penetrative oxidizing agent, has garnered significant attention as an antimicrobial agent for oil processing, preservation, and treatment (Guo et al., 2021). O_3 achieves this by electrophilically attacking the 8,9-unsaturated terminal furan ring, resulting in the formation of primary ozonides and subsequent monozonide derivatives such as ketones, aldehydes, and organic acids (Song et al., 2024). Ozone exposure duration and the moisture content of the oily food matrices influence the efficiency of ozonolysis. Because moisture in the samples facilitates the cleavage of additional furan/lactone rings due to the thermolysis of H_2O when subjected to heat. The thermolysis process generates H_3O^+ and OH^- groups that interact with the C_8-C_9 in the furan ring, leading to the lactone ring's opening and the $-CO_2H$ groups' formation (Luo et al., 2014). Significantly, O_3 at a concentration of 6.0 mg L^{-1} for 30 min reduced 65.9 % AFB1 levels from peanut oil without significantly altering AV, PV, polyphenol content, or RV (Chen et al., 2014).

EOW employs an electrolytic cell containing a membrane that separates the cathode and anode, producing two types of water: AlEW (alkaline electrolyzed water) and AEW (acidic electrolyzed water). Fan et al. (2013) tested the three kinds of AlEW at varying pH levels (10.5, 11.7, and 12.2). Under optimal conditions, using 10 mL of AlEW at 20 °C and pH 12.2, the complete removal of 40 μg kg^{-1} AFB1 was achieved from olive and peanut oils within 5.0 min. This method offers several merits, including antifungal/antibacterial properties, a simple design, low operational cost, no toxic chlorine compounds, and high environmental compatibility. Unlike other chemical methods, which often fail to meet necessary safety standards, electrolyzed water treatment poses

Table 1
An overview of the methods applied in removing AFB1 from edible oils.

Method	System [Concentration]	Type of oil [AFB1 dose]	Efficiency (%)	Comments	Reference
Physical	TiO_2 photocatalysis	Peanut	99.4≤	• T: 25 °C • *t*: 4.0 min • UV: 920 W m^{-2} • Visible: 2000 W m^{-2} • Power: 500 W • ROS[a]: $^{\bullet}OH$ and $O_2^{\bullet-}$ • AM[b]: HPLC-FLD[c]	Magzoub et al. (2019)
	UV–vis/MGO[d]/TiO_2 [10.0 mg]	Corn [200 μg kg^{-1}]	96.40	• T: 25 °C • *t*: 120 min • ROS: $^{\bullet}OH$ and h^+ • AM: HPLC-FLD	Sun et al. (2021)
	MGO/TiO_2-aptamer [8.0 mg]	Peanut [40.0 μg kg^{-1}]	77.30	• *t*: 30–120 min • Mercury lamp: 130 W • ROS: $^{\bullet}OH$, $O_2^{\bullet-}$, and h^+ • AM: HPLC	Ku et al. (2024)
	UV/I-STF[e] [0.1 M]	Peanut	81.96	• pH: 3.0, 7.0 • *t*: 120 min • UV: 26.0 μmol $m^{-2}s^{-1}$ • AM: ELISA[f]	Xu, Ye, Cui, Zhang, and Liang (2019)
	Visible-light/5-MAPI[g]	Vegetable [200 μg L^{-1}]	95.0	• *t*: 100 min • ROS: $^{\bullet}OH$, $O_2^{\bullet-}$, and h^+ • AM: UHPLC-MS[h]	Meng et al. (2024)
	UV	Peanut	96.00	• T: 26 °C • *t*: 30 min • UV: 55–60 mW cm^{-2} • P: 100 W • λ: 365 nm • AM: HPLC	Mao et al. (2016)
	UV	Peanut	100	• T: 8 ± 2 °C • *t*: 30 min • UV: 800 μW cm^{-2} • AM: HPLC	Liu et al. (2011)
	UV	Peanut [51.96 μg kg^{-1}]	86.08–88.74	• T: 25 °C • *t*: 10–40 min • UV: 6.4 mW cm^{-2} • P: 36 W • λ: 365 nm • AM: HPLC	Diao, Shen, et al. (2015)
	UV-LED	Groundnut	99.0	• T: 25 °C • *t*: 20 min • UV-LED: 3500 μW cm^{-2} • AM: HPLC	Wang et al. (2020)
	UV-LED cold-light	Peanut	~80.0	• *t*: 5 min • AM: UPLC-MS/MS	Wang et al. (2023)
	Solar radiation	Coconut [4.01–67.62 μg kg^{-1}]	>90.0	• T: 25 °C • *t*: 10 min • Solar: 971 ± 29.1 W m^{-2}	(Thimuthu kasun and Vanniarachchy, 2023)
	CN/GO/SA[i] [32.0 mg]	Peanut [200 μg kg^{-1}]	~98.4	• T: 25 °C • *t*: 120 min • Halide lamp: 130 w • ROS: h^+ and $O_2^{\bullet-}$ • AM: UPLC/MS	Sun, Yang, et al. (2023)
Chemical	Alkali-refining	Peanut [34.78 μg kg^{-1}]	98.94	• T: 43.51–77.07 °C • [Excess alkali]: 0.30 % • [NaOH]: 23.42 % • AM: HPLC	Ji et al. (2016)
	AlEW[j] [10.0 mL]	Vegetable [40.0 μg kg^{-1}]	~100	• T: 20 °C • pH: 12.2 • *t*: 5 min • ORP[k]: 861 mV • AM: LC-MS[l]	Fan et al. (2013)
	O_3 [50.0 mg L^{-1}]	Peanut [189.5 μg kg^{-1}]	89.40	• T: 25 °C • pH: 7.0 • *t*: 60 h • Flow rate: 5.0 L min^{-1}	(Diao et al., 2013)
Biological	*Aspergillus luchuensis* YZ-1	Vegetable [1.0 mg mL^{-1}]	~80.0	• T: 20–52 °C • pH: 3.2–8.2 • *t*: 120 min • Q_{max}: 46.57 mg g^{-1} • AM: HPLC	Zhang et al. (2024)
Physicochemical	Lac NF-P[m] [0.5 mg]	Peanut [50–150 μg kg^{-1}]	90.80	• T: 25 °C • *t*: 240 min	Lu et al. (2023)

(*continued on next page*)

Table 1 (*continued*)

Method	System [Concentration]	Type of oil [AFB1 dose]	Efficiency (%)	Comments	Reference
	HMMT-1[n]	Peanut [53.0 μg kg^{-1}]	100	• AM: HPLC • T: 25 °C • pH: 1.0 • *t*: 5–10 min • Q_{max}: 1.417 mg g^{-1}	Zhang et al. (2022)
	Fe_3O_4@ATP[o] [3.0 mg]	Peanut [33.83 μg kg^{-1}]	86.80	• AM: HPLC • T: 50.0 °C • *t*: 60 min • Q_{max}: 0.0529 mg g^{-1}	Ji and Xie (2021)
	MGO [10.0 mg]	Rice bran [16.1 μg L^{-1}]	96.4	• AM: HPLC • T: 37.0 °C • *t*: 40 min • Q_{max}: 1480 μg g^{-1}	Ji and Xie (2020)
	MCM[p]-41 [1.0 mg mL^{-1}]	Peanut [250 ng mL^{-1}]	80.35	• AM: HPLC • T: 25.0 °C • *t*: 120 min • Q_{max}: 215.93 ng mg^{-1}	Li, Wang, et al. (2022)
	MOF-235[q] [5.0 mg]	Vegetable [50.0 μg kg^{-1}]	96.7	• AM: HPLC • T: 24.0 °C • *t*: 30 min • Q_{max}: 9.0 mg g^{-1}	Du et al. (2023)
	0.15 % CS/SDS/AC[r]	Peanut [73.53 μg kg^{-1}]	92.40	• AM: UPLC-MS/MS • T: 70.0 °C • *t*: 40 min • Q_{max}: 34.530 μg g^{-1}	Ji et al. (2025)
	0.2 % SAC[s]	Peanut [58.89 μg kg^{-1}]	93.5	• AM: HPLC • T: 40.0–90.0 °C • *t*: 120 min • Q_{max}: 0.068 mg g^{-1}	Jiang et al. (2023)
	Eucheuma cottonii fiber	Peanut	–	• AM: HPLC • T: 25.0–70.0 °C • *t*: 60 min • Q_{max}: 0.789 mg g^{-1}	Guo et al. (2022)
	Fe-BTC@Lac@FB[t] [0.79 g L^{-1}]	Peanut [1.0 ppm]	>90.0	• AM: HPLC • T: 25.0 °C • *t*: 60 min • Q_{max}: 11.2 mg g^{-1}	Rasheed, Ain, and Liu (2024)
	0.45SDB-6-K-9[u]@Fe_3O_4 [50.0 mg]	Peanut [200 ng mL^{-1}]	~70.0	• AM: HPLC • T: 65.0 °C • pH: 7.0 • *t*: 120 min	Ying et al. (2023)
	Cu-BTC MOF [30.0 mg]	Corn/Peanut [5.0 μg mL^{-1}]	90.0	• AM: HPLC • T: 25.0 °C • pH: 7.0 • *t*: 30 min • Q_{max}: 16.67 mg g^{-1}	Ma et al. (2021)
	VC-rGO/Fe_3O_4[v] [5.0 mg]	Vegetable [50.0 μg kg^{-1}]	>90.0	• AM: HPLC-FLD • T: 25.0 °C • *t*: 40 min • Q_{max}: 0.352 μg mg^{-1}	Ma et al. (2024)
	MRHB[w] [5.0–30.0 mg g^{-1}]	Peanut [10.0 μg mL^{-1}]	>95.0	• AM: HPLC • T: 45.0 °C • pH: 7.0 • *t*: 60 min • Q_{max}: 951.1 μg g^{-1}	Li et al. (2023)
	FM@GO@Fe_3O_4[x] [15.0 mg]	Vegetable [50.0 μg kg^{-1}]	>70.0	• AM: UPLC-MS/MS • T: 50.0 °C • *t*: 600 min • Q_{max}: 0.3533 μg mg^{-1}	(Ma et al., 2023)
	MCNP[y] [4.4 mg L^{-1}]	Palm [0.0491 μg L^{-1}]	94.87–100	• AM: LC-MS • T: 30.0 °C • *t*: 30 min	Aringbangba et al. (2021)
	PDA@Fe_3O_4-MWCNTs[z] [50 mg]	Vegetable [1.0 μg L^{-1}]	70.0–90.0	• AM: HPLC • T: 25 °C • pH: 7.0 • *t*: >10 min	Xu et al. (2021)
	BF-NH_2-Lac[2]	Corn [1.0 mM $μg^{-1}$]	>90.0	• AM: MSPE[1]/HPLC/FLD • T: 30 °C • pH: 7.0 • *t*: 300 min	Rasheed, Ain, Ali, and Liu (2024)
	PL-GO_x- Fe_3O_4@COF[3] [0.75 mg mL^{-1}]	Vegetable [40.0 μg kg^{-1}]	100	• AM: HPLC-FLD • T: 25 °C • *t*: 360 min	Fu et al. (2024)
	DC/CFOS NC[4] [2.5 mg L^{-1}]	Corn [50.0 μg mL^{-1}]	97.40	• AM: HPLC • T: 25 °C	Abasi et al. (2023)

(*continued on next page*)

Table 1 (*continued*)

Method	System [Concentration]	Type of oil [AFB1 dose]	Efficiency (%)	Comments	Reference
	PDA-PS NFsM[5] [2.5 mg]	Edible [50.0 μg L^{-1}]	84.80–86.50	• pH: 7.0 • *t*: 100 min • Q_{max}: 3.106 mg g^{-1} • T: 25.0 °C • pH: 7.0 • *t*: 60 min • AM: UPLC-MS/MS	Dai et al. (2022)

[a] Reactive oxygen species.
[b] Analysis method.
[c] High performance liquid chromatography- Fluorescence detection.
[d] Magnetic graphene oxide.
[e] Iodine doped supported TiO_2 thin film.
[f] Enzyme-Linked Immunosorbent Assay.
[g] Silver phosphotungstate/polyimide.
[h] Ultra high performance liquid chromatography-mass spectrometry.
[i] A porous graphitic carbon nitride/graphene oxide hydrogel microsphere.
[j] Alkaline electrolyzed water.
[k] Oxidation-reduction potential.
[l] Liquid chromatography-mass spectrometry.
[m] Amphipathic laccase-inorganic hybrid nanoflower.
[n] Montmorillonite modified with histidine.
[o] Magnetic attapulgite.
[p] Rice husk-based mesoporous silica.
[q] Metal-organic framework.
[r] Activated carbon co-modified by chitosan and sodium dodecyl sulfate.
[s] Activated carbon functionalized with sodium dodecyl sulfonate.
[t] Fe-MOF-laccase-magnetic biochar.
[u] Magnetic soybeans dreg-based biochar.
[v] Synthesized Fe_3O_4/reduced graphene oxide composite using vitamin C.
[w] Magnetic rice husk-based biochar.
[x] A hierarchical fungal mycelia@graphene oxide@Fe_3O_4,
[y] Magnetic chitosan nanoparticles.
[z] Polydopamine-coated magnetic multi-walled carbon nanotubes.
[1] Magnetic solid-phase extraction.
[2] Laccase immobilized on NH_2-activated magnetic biochar.
[3] Amphipathic enzyme-metal hybrid nanoreactor with covalent organic frameworks.
[4] Dopamine-loaded biomass chitosan-iron-cobalt spinel oxide nanocomposite.
[5] Polydopamine modified nanofibers membrane.

no poisonous residues or environmental hazards, making it a sustainable and safe alternative for oil refining processes (Guo et al., 2021).

3.3. Biological methods

This technique involves the microbial/enzymatic conversion of AFB1 into non-toxic or less toxic metabolites. Numerous microorganisms originating from diverse sources, including animal waste, water, soil, and even contaminated food products, have been documented to possess the ability to degrade AFB1 (An et al., 2024). Extensive studies on the biodegradation of AFB1 in oily matrices have not been conducted thus far due to the various challenges (*e.g.,* denaturation, inefficiency of electron transfer, and hydrolysis enzymes in oily matrices, and limited contact surface and accessibility between lipophilic AFB1 and hydrophilic enzymes) (Rasheed, Ain, & Liu, 2024). Zhan et al. (2024) revealed that *Aspergillus luchuensis* YZ-1 possesses a remarkable capacity to adsorb AFB1, marking the first instance of such an ability. The interaction between AFB1 and YZ-1 is characterized by high stability. Notably, spores demonstrated superior adsorption efficiency compared to *mycelia*, successfully adsorbing nearly 95.0 % of AFB1 within 15.0 min. The adsorption capacity of the spores reached an impressive 46.57 mg g^{-1}. Additional investigations suggest that proteins within the spores are crucial to the adsorption mechanism. When spores are utilized in vegetable oil for AFB1 adsorption, they exhibit effective adsorption properties while preserving their quality. Indeed, the lack of substantial differences in the appearance of vegetable oils, including corn and soybean oil, were demonstrated before and after spore adsorption, along with the results obtained from FT-IR and GC-MS analyses. The lack of changes in chemical structure (as evidenced by the approximate similarity of peak patterns) and the composition of saturated and unsaturated fatty acids before and after spore treatment supports this claim. Given that the high viscosity of oil matrices reduces the diffusion rate and consequently the adsorption rate of spores in oils compared to aqueous environments, the spores adsorbed ~70.0 % AFB1 from corn and soybean oils, which increased to 80.0 % after 120 min (Zhang et al., 2024).

3.4. Physicochemical methods

Physicochemical techniques mainly rely on adsorption and create various interactions, including electrostatic- and H-bonding, hydrophobic/hydrophilic, n-π, and π-π interactions, between AFB1 and the adsorbent (Kolarič et al., 2024; Moradian et al., 2024). In general, adsorbents are classified as bio-binders (*e.g.,* chitosan, cellulose, rice husk, activated carbon, various biochar, etc.) and traditional organic/inorganic binders (*e.g.,* montmorillonite, attapulgite, etc.), which are widely used for the removal of AFB1 from oily matrices (Vila-Donat et al., 2018). Zhang et al. (2022) reported that histidine-modified montmorillonite under highly acidic conditions (HMMT-1) exhibited the highest adsorption capacity for AFB1 from peanut oil (1.417 mg g^{-1}) at pH 1.0 compared to pH 2.0 and 4.0. The enhanced performance is attributed to several factors, including a notable increase in specific

surface area due to particle size reduction, more effective grafting of protonated histidine into the interlayer structure, improved mesoporous structure, and enhanced chemical interactions between AFB1 and the functional groups of histidine. Furthermore, thermodynamic data showed that the ΔG value for HMMT-1 was more negative than other variants (*e.g.,* - 6.36 at 383 K), indicating that the adsorption process was spontaneous and accompanied by increased entropy. At pH < 7.0 (high H^+ concentration), the adsorbent surface may become protonated, which subsequently affects the adsorbent-AFB1 interaction/propensity, AFB1 solubility, and the surface properties of the adsorbent. In contrast, at pH > 7.0, the adsorbent and AFB1 molecules may be negatively charged, leading to electrostatic repulsion, which reduces adsorption. Besides, the excellent adsorption performance (86.82 %) of the Fe_3O_4@attapulgite magnetic composite from contaminated peanut oils with minimal sterol nutrient and V_E loss can be attributed to its abundant micro-pore structure, large specific surface area, and significant negative surface dipole density (Table 1) (Ji & Xie, 2021). Increasing temperature generally tends to lower oil viscosity, enhancing the mass transfer rate and improving AFB1 removal performance. Moreover, as the initial AFB1 concentration increases (<33.83 μg kg^{-1}), the likelihood of AFB1 interacting with the adsorbent also rises. Nevertheless, if the initial concentration is excessively high (>33.83 μg kg^{-1}), the available adsorption sites of the supermagnetic composite may become saturated, reducing AFB1 removal efficiency. Interestingly, this process not only enhanced the quality of the oil by adsorbing pigments and diminishing the PV but also significantly preserved the nutritional components (Ji & Xie, 2021). The amphipathic laccase that coats the surface of the hybrid nanoflower (Lac NF-P) is crucial for holding the moisture of Lac within the two-phase system (O/W), which is essential for the micro-environment of adsorption site and direct/indirect electron transfer during the enzymatic detoxification of AB1 from peanut oil (Lu et al., 2023). Consequently, Lac NF-P demonstrated significant performance and improved stability in the AFB1 bio-removal from peanut oil. When Lac NF-P was employed as the bio-adsorbent, AFB1 levels were reduced to below 0.96 μg kg^{-1} within 3.0 h, with initial AFB1 concentrations varying from 50 to 150 μg kg^{-1}. As depicted in Table 1, various absorbents derived by chitosan, cellulose, rise husk, chitosan-dopamine, NH_2-activated magnetic biochar, magnetic polydopamine, and polydopamine modified nanofibers membrane have high adsorption capacity due, mainly, to the high specific surface area, presence of plentiful adsorption sites and micro-sized pores.

To evaluate and compare the AFB1 removal efficiency of various adsorbents from edible oils, particularly peanut oil, five selected adsorbents, including Lac NF–P, Eucheuma cottonii fiber, MCM-41, Fe-BTC@Lac@FB nanocomposite, and Cu-BTC MOF were assessed under similar laboratory conditions (ambient temperature, pH 6.0–7.0, and peanut oil matrix). Structurally, Lac NF–P is a bio-enzymatic adsorbent based on laccase immobilized on a natural polymer, classified as a biocatalytic detoxifying material. It successfully reduced AFB1 levels to below 0.96 μg kg^{-1} within 240 min without compromising oil quality. Notably, it retained over 80.0 % of its enzymatic activity after five consecutive reuse cycles, indicating good recyclability (Lu et al., 2023). Eucheuma cottonii fiber is a natural plant-based adsorbent derived from red seaweed. While its adsorption capacity is moderate (~0.789 mg g^{-1}), it offers ultra-fast adsorption (equilibrium within 15 min) and is fully biodegradable and food-safe (Guo et al., 2022). MCM-41, a mesoporous silica nanostructured adsorbent, is known for its very high specific surface area and regular porous structure, with excellent thermal and chemical resistance. However, its lower adsorption capacity (0.21593 mg g^{-1}) and longer equilibrium time (24 h) limit its suitability for rapid or industrial-scale applications (Li, Liu, et al., 2022). Fe-BTC@Lac@FB is a nanocomposite combining a metal-organic framework, a laccase enzyme, and a fibrous support. This adsorbent exhibits high adsorption capacity (11.2 mg g^{-1}), an appropriate equilibrium time (60 min), and is compatible with peanut oil. Reports indicate successful recyclability for up to five cycles with less than 15.0 % reduction in adsorption performance, indicating high chemical, thermal, and storage stability. Moreover, Fe-BTC@Lac@FB does not adversely affect peanut oil quality and is safe regarding cytotoxicity results (Rasheed, Ain, & Liu, 2024). Finally, Cu-BTC MOF, a metal-organic framework composed of copper and organic ligands, can remove over 90.0 % of AFB1 (16.67 mg g^{-1}) within 30 min. Its porous structure, ease of synthesis, and low cost make it a favorable candidate for rapid toxin removal in industrial-scale operations (Ma et al., 2021). Under identical experimental conditions, Cu-BTC MOF and Fe-BTC@Lac@FB demonstrated superior adsorption efficiency, reusability, and scalability, making them more suitable for industrial applications. In contrast, Lac NF–P and Eucheuma cottonii fiber offer excellent biosafety and applicability in food or pharmaceutical scenarios. MCM-41, while stable and reusable, may be better suited for slower, controlled processes. The findings present the maximum absorption capacity: Cu-BTC MOF > Lac NF–P ~ Fe-BTC@Lac@FB > Eucheuma cottonii fiber > MCM-41. Ultimately, the final adsorbent selection should consider the specific application needs, recyclability, biosafety, and economic aspects.

3.5. Novel approaches based on nanozymes

Natural enzymes extracted from biological sources are costly to manufacture and store and are highly sensitive to temperature, pH, and ecological conditions. In contrast, nanozyme structures address these limitations by allowing optimization of their properties through modifications in size, shape, chemical composition, and surface characteristics, ensuring their long-term usability with high bio-stability and high tunable catalytic activities. Consequently, nanozymes can serve as substitutes for natural enzymes by mimicking/simulating activities such as peroxidase, oxidase, catalase, and superoxide dismutase (Nagendran et al., 2024; Meng et al., 2020; Wang et al., 2023; Naveen Prasad, Bansal, & Ramanathan, 2021). Nanozymes are classified into several categories based on their catalytic activities and compositions, such as single-atom active sites nanozyemes (*e.g.,* Fe, Pd, and Co) and multi-metallic active site nanozymes (*e.g.*, Fe-Mn, Fe-Pd, Au-Ir, and Co-Fe) (Table 2) (Demkiv et al., 2021).

Peroxidase-like nanozymes have explicitly been utilized in the food industry to remove AFB1 from edible oils. This section examines the features, mechanisms, merits/demerits, and challenges of peroxidase-based nanozymes. Peroxidase-like nanozymes mimic the activity of natural peroxidase enzymes by catalyzing oxidation reactions using H_2O_2 as an oxidizing agent. Nanozymes based on metal oxides, or more specifically metal-organic frameworks (MOFs), represent a new class of hybrid and porous materials designed for AFB1 removal through adsorption and separation/peroxidase-like mechanisms (Dey et al., 2014; Wei et al., 2023).

MOFs enhance enzyme stability by embedding natural enzymes into their pores and shells. In this method, the MOF serves solely as a carrier or protector, and the presence of natural enzymes is essential. Also, it acts as an artificial (biomimetic) enzyme without requiring the presence of natural enzymes. Thus, in a study by Ren et al. (2019), three peroxidase-like MOFs (MIL-x, x = 53, 68, and 100) were compared to remove AFB1. The experiments demonstrated that the removal of AFB1 by MOFs occurred through adsorption and/or catalysis. MIL-68 exhibited the most substantial adsorption among the three MOFs, while MIL-53 demonstrated the highest catalytic activity due to its combined peroxidase/Fenton characteristics and high Fe amounts. The adsorption capacity depended on the pore size and structure of the MOFs. MIL-68, with larger pores and a 2D structure, provided greater access to AFB1 molecules, whereas the 3D structure of MIL-100 resulted in more complex molecular pathways and reduced adsorption capacity. In MIL-53, its flexible framework hindered the transfer of AFB1 molecules.

Additionally, the MOFs could efficiently remove AFB1 in complex matrices such as cellulose, zein, starch, and corn oil. Although zein slightly reduced the adsorption capacity, it enhanced the catalytic activity of MIL-68, maintaining an almost constant overall removal

Table 2
AFB1 removal by enzymatic-like technologies.

Nanozyme [dose]	Sample [AFB1 dose]	Oxidant [Concentration]	Efficiency (%)	Comments	Reference
MF@CRHHT[a] [0.4 g L^{-1}]	Aqueous [100 ng L^{-1}]	PMS[b] [0.8 mM]	99.30	• T: 25 °C • pH: 5.0–9.0 • *t*: 20 min • ROS[c]: $SO_4^{\bullet-}$, $^{\bullet}OH$, $^{\bullet}O_2^-$, and $^1O_2$ • AM[d]: HPLC	Faraji et al. (2023)
MF@CRHHT [0.4 g L^{-1}]	Aqueous [100 ng L^{-1}]	PDS[e] [1.0 mM]	45.90	• T: 25 °C • pH: 5.0–9.0 • *t*: 180 min • AM: HPLC	Faraji et al. (2023)
MF@CRHHT [0.4 g L^{-1}]	Aqueous [100 ng L^{-1}]	H_2O_2 [5.0 mM]	91.10	• T: 25 °C • pH: 5.0–9.0 • *t*: 60 min • AM: HPLC	Faraji et al. (2023)
Pd@PCN-222[f] [1.2 mg L^{-1}]	Corn oil [2.5 μg mL^{-1}]	H_2O_2 [5.0 mM]	85.36	• T: 25 °C • pH: 7.0 • *t*: 120 min • ROS: $^{\bullet}OH$ • AM: HPLC	Wei et al. (2022)
Co_2N@Co-N_4[g] [0.4 g L^{-1}]	Water	H_2O_2 [1.0 M]	100	• T: 25 °C • pH: 3.0–8.0 • *t*: 180 min	Ouyang et al. (2022)
Fe_3O_4/ZIFs[h] [7.0 mg]	Water	PMS [0.3 mM]	97.40	• T: 25 °C • pH: 3.0–8.0 • *t*: 30 min • AM: HPLC	Zhang et al. (2022)
SSM/CoF/Au@Ir[i]	Peanut, corn, and wheat [0.5 μg mL^{-1}]	H_2O_2 [0.1 M]	81.14	• pH: 3.5 • *t*: 120 min • Xenon lamp: 300 W	Zhou et al. (2024)
Fe-MIL-53[j] [0.1 g L^{-1}]	Water [1000 ppb]	H_2O_2 [20.0 mM]	100	• T: 40 °C • pH: 4.0 • *t*: 2400 min • AM: HPLC	Ren et al. (2019)
Fe/N-PC[k] [0.25 mg]	Water	PMS [1.0 mM]	99.88	• T: 25 °C • pH: 3.0 • *t*: 30 min • AM: HPLC-FLD	Zhang et al. (2022)
Pd@CRH-400[l] [1.0 g L^{-1}]	Edible oil [10.0 μg mL^{-1}]	H_2O_2 [4.0 mM]	89.10	• T: 25 °C • pH: 2.0–10.0 • *t*: 120 min • ROS: $^{\bullet}OH$, $^{\bullet}O_2^-$ • AM: HPLC	Zabeti et al. (2024)
Pd@CRH-400 [1.0 g L^{-1}]	Water [10.0 μg mL^{-1}]	H_2O_2 [4.0 mM]	97.80	• T: 25 °C • pH: 2.0–10.0 • *t*: 120 min • AM: HPLC	Zabeti et al. (2024)
MIL-100[m] [0.1 g L^{-1}]	Water [1000 ppb]	H_2O_2 [20.0 mM]	85.0	• T: 40 °C • pH: 4.0 • *t*: 480 min • AM: HPLC	Ren et al. (2019)
Fe_3O_4/GO/NH_2-MIL-53(Fe) [5.0 mg]	Water [50.0 mg L^{-1}]	H_2O_2 [2.0 mM]	99.0	• *t*: 60 min • pH: 3.0 • T: 25 °C • ROS[2]: $^{\bullet}OH$, $^{\bullet}O_2^-$, and $^1O_2$ • AM: HPLC	Wang et al. (2025)

[a] Dual metal oxides Mn-Fe anchored in/on (chitosan/rice husk waste/hercynite hybrid nanoparticles.
[b] Peroximonosulfate.
[c] Reactive oxygen species.
[d] Analysis method.
[e] Peroxidisulfate.
[f] Fe-tetrakis (4-carboxyphenyl) porphyrin and Pd.
[g] Nitrogen-encapsulated Co_2N clusters coupled with isolated Co-N_4 moieties.
[h] Zeolitic imidazolate frameworks.
[i] A donor-acceptor covalent organic framework bound on to the surface of stainless-steel mesh.
[j] Fe(III)-based metal-organic frameworks.
[k] Fe/N-codoped porous carbon.
[l] Magnetic Pd-chitosan/glutaraldehyde/rice husk/hercynite composite.
[m] Metal-organic frameworks based enzymes.

efficiency. Thus, MIL-68 could act as an effective anti-interference buffer. In the adsorption process, the high hydrophobicity and nonpolar nature of AFB1 molecules played a key role, with π-π interactions and hydrophobic adsorption being the main contributors. The influence of temperature, the amount of H_2O_2, and pH on the efficiency of AFB1 removal was also examined systematically. The adsorption efficiency of the mentioned MOFs remained stable over a wide temperature range (30–60 °C), while the catalytic performance increased with rising temperatures. This observation indicates that the catalytic performance of MOFs is more responsive to temperature variations than their adsorption capabilities. Notably, MIL-68 displayed insensitivity to temperature fluctuations due to its predominant adsorption characteristics. Results validated that hybrid bi- or trimetallic nanozymes could display a higher AFB1 detoxification performance than the single-metal nanozyme, which can be related to the synergistic effects of multi-metallic-based nanozymes. This synergism can boost electron transport efficiency and subsequently amplify the detoxification efficiency.

Furthermore, the catalytic performance of mentioned MOFs showed a positive correlation with the concentration of H_2O_2, with 20 mM identified as an optimal concentration for AFB1 removal in peroxidase-like MOFs. Additionally, MOFs' adsorption and catalytic capacities diminished as pH increased, suggesting that a slightly acidic environment enhances AFB1 removal, akin to the behavior of natural peroxidase (Jiang et al., 2019). In another study, Wei et al. (2022) synthesized MOFs with varying central metals to assess their adsorption capabilities, specifically identifying MOF(Fe) as PCN-222. The efficiencies recorded were 56.97 % (MOF(Ce)), 54.32 % (MOF(Zn)), and 56.32 % (PCN-222), in contrast to 38.41 % for Pd@PCN-222. This reduction in efficiency may be attributed to the occupation/blocking of some adsorptive centers on the surface of PCN-222 by Pd NPs.

Additionally, analysis of the N_2 adsorption isotherm revealed a decrease in both the specific surface area and pore size of Pd@PCN-222. Following this, H_2O_2 was introduced into the adsorption system of the MOFs and AFB1, leveraging the enzyme-mimicking performance of PCN-222. In comparison to PCN-222 and Pd@PCN-222, MOF(Ce) and MOF(Zn) demonstrated lower catalytic efficiency due to their lack of peroxidase-mimicking properties, with the addition of H_2O_2 adversely affecting their available adsorptive centers. The removal efficiencies for PCN-222 and Pd@PCN-222 improved by 19.94 % and 46.81 %, respectively. Furthermore, it is well established that the Fe-TCPP ligand and Pd centers significantly contribute to peroxidase-mimicking activities (Ling et al., 2017). Consequently, the removal efficiency of Pd@PCN-222 surpassed that of the other MOFs, leading to its selection for AFB1 removal in corn oil. It also demonstrated high stability and reusability, maintaining a removal efficiency >91.0 % over five consecutive cycles with only a slight decline in performance. Since no metal leakage, including Pd and Fe, was observed in the oil after treatment. In addition, Zabeti et al. (2024) presented another type of process based on nanozyme peroxidase called Pd@CRH-400 (chitosan-rice husk) to remove AFB1 from edible oils. The findings demonstrated that the H_2O_2/Pd@CRH-400 system effectively detoxified AFB1 by approximately 89.53 % in oily matrices. The observed reduction in detoxification percent in oil, as opposed to water, can be attributed to the presence of fatty acids (*e.g.,* C16:0, C18:1, and C18:2), which tend to adhere to the surface of Pd@CRH-400, thereby obstructing the active centers necessary for the AFB1 removal. Furthermore, the Pd@CRH-400 biocomposite maintained its performance over at least seven cycles, exhibiting a removal efficiency of 96.1 % with negligible structural changes. The apparent reaction rate constant (k_{obs}) was recorded at 4.65 $\times 10^{-3}$ min^{-1}. According to ICP-OES analysis, the leaching of Pd into the aqueous medium after seven cycles was only 0.0187 mg L^{-1}, which is considered negligible. The slight decrease in performance observed in the eight cycles was attributed to factors including surface oxidation by H_2O_2, accumulation of intermediate products, and particle size growth.

In Table 2, all types of processes based on nanozyme peroxidase in the presence of H_2O_2 and other oxidants in oily and aqueous matrices have been investigated. While nanozymes demonstrate significant advantages and strengths in eliminating AFB1, they face specific challenges and limitations, particularly in oily matrices. The reduced efficiency of peroxidase nanozymes in removing AFB1 in oil matrices can be attributed to the physicochemical properties of oils and the mechanism of action of nanozymes. Peroxidase nanozymes generally exhibit high activity in hydrophilic (aqueous) environments, as their catalytic reaction depends on the H_2O-H_2O_2 interaction (Su et al., 2022). Also, due to their hydrophobic nature, oils can hinder the diffusion of H_2O_2 and its accessibility to the nanozyme surface, thereby reducing catalytic activity. The produced $^{\bullet}OH$, $O_2^{\bullet-}$ are more stable in polar environments like water and can effectively react with AFB1. However, in oily matrices, the stability and diffusion of these radicals are diminished due to the nonpolar nature of the oil, resulting in reduced efficiency of AFB1 removal (Demkiv et al., 2021). For the nanozymes and AFB1 to interact effectively, they must be uniformly distributed in the matrix. In oil matrices, the oil's high viscosity and adhesive properties can prevent sufficient interaction between nanozymes, H_2O_2, and AFB1, directly impacting the efficiency of the process (Zhang et al., 2022). Edible oils contain free fatty acids, triglycerides, and natural antioxidants. These compounds can react with the ROS generated by the nanozymes, reducing the concentration of effective radicals available to degrade AFB1.

Furthermore, peroxidase nanozymes may become inactivated due to the adsorption of fatty materials onto their surface (fouling or surface coating). This process can reduce the active surface area of the nanozymes and their ability to generate active radicals (Su et al., 2022). All these factors collectively contribute to the reduced efficiency of peroxidase nanozymes in oily matrices.

The chemical mechanism of action of peroxidase-like nanozymes is based on their ability to catalyze oxidation reactions in the presence of H_2O_2. Specifically, the nanozyme as an activator facilitates the decomposition of H_2O_2 into highly oxidative species, which attack the AFB1 and induce its oxidation (Zhang et al., 2022). This key step is affected by the unique nanozyme structure and peroxidase-like reaction conditions.

The surface of the metallic or metallic oxide-based nanostructure possesses unique characteristics, such as active metal centers (*e.g.,* Fe^{3+} and Pd^0) that enable crucial electron transfer between H_2O_2 and AFB1. The electron-rich multi-metallic nanozymes can facilitate the transfer of electrons from H_2O_2 more than single-metallic nanozyme, resulting in the facile disruption of the -O-O- bond and more generation of $^{\bullet}OH$ (eqns. (1)–(3)).

$$\equiv M^{(n-1)+} + H_2O_2 \rightarrow \equiv M^{n+} + HO^- + {}^{\bullet}OH \quad (1)$$

$$\equiv M^{n+} + H_2O_2 \rightarrow \equiv M^{(n-1)+} + HO^- + {}^{\bullet}OH \quad (2)$$

$$\equiv M^{n+} + H_2O_2 + H^+ \rightarrow \equiv M^{(n-1)+} + H_2O + {}^{\bullet}OH \quad (3)$$

$$\equiv M^{(n-1)+} + H_2O_2 \rightarrow \equiv M^{n+} + 2\,H^+ + {}^{\bullet}O_2H \quad (4)$$

$$\equiv M^{n+} + H_2O_2 \rightarrow \equiv M^{(n-1)+} + 2\,H^+ + O_2^{\bullet-} \quad (5)$$

$$\equiv M^{(n-1)+} + H_2O_2 \rightarrow \equiv M^{n+} + 2\,H^+ + O_2^{\bullet-} \quad (6)$$

$$\equiv M^{(n-1)+} + O_2 \rightarrow \equiv M^{n+} + O_2^{\bullet-} \quad (7)$$

$$\equiv M^{n+} + O_2^{\bullet-} + H_2O_2 \rightarrow \equiv M^{(n-1)+} + O_2 + HO^- + {}^{\bullet}OH \quad (8)$$

$$O_2^{\bullet-} + H_2O_2 \rightarrow O_2 + OH^- + {}^{\bullet}OH \quad (9)$$

$$\equiv M^{n+} + H_2O_2 \rightarrow \equiv M^{(n-1)+} + H^+ + {}^{\bullet}O_2\,H \quad (10)$$

$$\equiv M^{n+} + H_2O_2 \rightarrow \equiv M^{(n-1)+} + H^+ + {}^{\bullet}O_2\,H \quad (11)$$

$$O_2 + e^- \rightarrow H_2O_2 \rightarrow 2\,{}^{\bullet}OH \quad (12)$$

$$HO_2^{\bullet} + H_2O_2 \rightarrow H_2O + {}^1O_2 + {}^{\bullet}OH \quad (13)$$

$$AFB1 + {}^{\bullet}OH/{}^{\bullet}O_2H/O_2^{\bullet-}/{}^{\bullet}OH_2 \rightarrow [\text{Intermediates}] \rightarrow \text{Transformed products.} \quad (14)$$

As exhibited in Fig. 2, the enzymatic-like catalytic pathway involves a redox cycle and electrons transfer to produce reactive oxygen species (*i.e.,* $^{\bullet}OH$, $O_2^{\bullet-}$, $^1O_2$ and $^{\bullet}O_2H$), and afterward the regeneration of $\equiv M^{(n-1)+}$ to $\equiv M^{n+}$ by the reduction with peroxide hydrogen and active species (eqns. (1)–(14)) (Faraji et al., 2023; Zabeti et al., 2024).

Given that food safety and quality are the primary criteria for eliminating AFB1 from food products, including edible oils, Table 3 comprehensively compares edible oils' physicochemical/nutritional properties after refinement using various processes.

4. Comparative study on the AFB1 removal mechanism from oily matrices with various technologies

Since the lactone, cyclopentanone, and the terminal C=C furan ring (responsible for forming the vinyl ether) are associated with toxicity, mutagenicity, and carcinogenicity, any structural modification of these moieties significantly reduces the toxicity of the degradation products. Table 4 comprehensively reviews all intermediates/byproducts and mechanisms associated with each method.

4.1. Physical mechanism

The reaction of free radicals (*i.e.,* $^{\bullet}OH$, $^{\bullet}H$), as well as hydrogen peroxide, are produced as a result of the destruction of the covalent bond of water molecules under the influence of cavitation by the ultrasound process (Castro-Ríos et al., 2021; Liu, Li, Liu, Bai, & Bian, 2019). Liu, Li, Liu, Bai, and Bian (2019) revealed two degradation pathways of AFB1 as follows: (*i*) demethylation and then through epoxidation and the addition of $^{\bullet}OH$ and $^{\bullet}H$ to the double bond of the terminal furan ring (**PP1**, **PP2**), and (*ii*) opening of the lactone ring through hydrolysis and oxidation after breaking the furan ring and producing **PP10-PP12** (Peng et al., 2023). The formation of **PP3**, **PP4**, **PP7**, **PP8**, **PP13**, **PP16**, and **PP17** through the electron beam method can be attributed to the production of abundant $^{\bullet}OH$, $^{\bullet}H$, and H_2O_2 under the reactions on the terminal C=C furan ring, O-CH_3 group, and also the opening of the lactone ring (Peng et al., 2023; Song et al., 2024). The hydrolysis of the lactone ring and the addition of the hydroxyl group to the terminal double bond to produce **PP14** and **PP15** by pulsed light were identified by Qi et al. (2023). In addition to the things mentioned concerning UV radiation, it is essential to note that due to its high potential and the production of many radicals, many products are produced during the degradation process, including **PP1**, **PP7-PP9,** and **PP13** (Song et al., 2024). As well as two products, **PP13** and **PP16,** were formed in the evaluation conducted by Wang et al. (2011) to destroy AFB1 by applying gamma radiation. Moreover, **P5** and **P6** are produced by the microwave process, which is accompanied by the hydrolysis of lactone and furan rings removal of COOH and OCH_3 (Shi, 2016; Zhang et al., 2021b).

4.2. Chemical mechanism

According to the research conducted by Diao et al. (2012), due to the ozonation of AFB1, highly oxidative products **CP3-CP7** were formed under the influence of oxidation, addition, electrophilic attack, and Criegee mechanism. Also, it should be noted that two products resulting from degradation with ozone, *i.e.,* **CP3** and **CP4**, were also observed in the physical degradation of AFB1 in peanuts with UV radiation, which suggests the possibility of ozone production in UV photolysis (Diao et al., 2012; Song et al., 2024). Luo et al. (2014) showed that compounds **CP1** and **CP2** were produced by the effects of ozone on the terminal double bond in the furan ring and O-CH_3 structure through hydration and hydroxylation. Therefore, the ozonation process can significantly reduce toxicity. It can be said that the presence of abundant hydroxyl groups in the structure of the products shows the strong oxidative effect of ozone on AFB1 (Luo et al., 2014; Song et al., 2024). In addition, **CP5-CP8** was obtained due to the degradation of AFB1 in corn oil using chlorine dioxide (ClO_2), among which compound **CP8** is much more toxic than AFB1 due to an epoxide ring. ClO_2, a potent oxidizing agent used as a food additive, has a lower cost and more straightforward operation than ozone (Yu et al., 2020).

On the other hand, Faraji et al. (2023) illustrated that H_2O molecules were absorbed on the surface of the activator, then Mn^{2+}-OH and Fe^{3+}-OH were formed and reacted with oxidant molecules, which led to the production of reactive species (*i.e.,* $^{\bullet}OH$, $SO_4^{\bullet-}$ and $O_2^{\bullet-}$ and $^1O_2$). These reactive species form **CP8** after attacking AFB1 and epoxidation of the terminal double bond of the furan ring, and then **CP9** is produced by ring opening and hydration process. Further, in another research, with the re-attack of these active species, **CP10-CP13** products are obtained through lactone ring opening, decarboxylation, demethylation, and hydroxylation, respectively.

4.3. Biological mechanism

BP1-BP4 and **BP6-BP12** products were produced by using crude extracellular enzymes extracted from *A. niger* and *Pleurotus ostreatus* co-

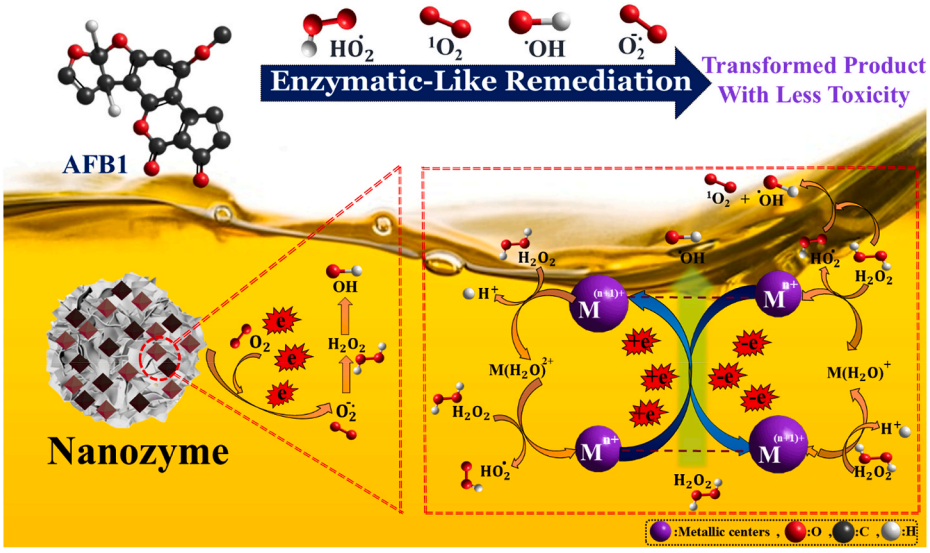

Fig. 2. Schematic diagram of enzymatic-like remediation pathway of AFB1 by nanozymes [where ≡ M represents the linkage of the active metallic center to 3D scaffold].

Table 3
Evaluation of nutritional/physicochemical properties changes in final detoxified oil samples.

Method	Type of oil	Nutritional properties	Physicochemical properties	Reference
TiO_2 photocatalysis	Peanut	• No change in saturated FAs[a] (C20:0[b], C16:0[c], C14:0[d], and C18:0[e]). • No change in unsaturated FAs (C18:2, n-6[f], C18:1, n-9[g], and C18:3, n-3[h]). • Changing the chemical composition of lipids in high doses of UV.	• No change in AV[i], PV[j], SV[k], MC[l], and RI[m]. • Significant incremental change in IV[n].	(Magzoub et al., 2018)
MGO/TiO_2	Corn	• Stability of unsaturated FAs.	• No change in SV and IV. • Increases in PV, AV, and *p*AV[o]. • No change in MC, IV.	(Sun et al., 2020)
UV-LED	Groundnut	• Stability of FAs composition.	No change in AV and PV.	Wang et al. (2020)
Gamma-ray	Soybean	• Increasing the relative content of C16:0 and C18:0. • Reducing the tocopherol content.	• Increasing of AV and PV. • Reduction of IV. • Decreased oxidation stability.	Zhang et al. (2018)
Visible/5-MAPI	Vegetable	• No change in FAs.	• Increasing of PV. • No change in AV.	Meng et al. (2024)
CN/GO/SA	Peanut	• No change in un/saturated FAs.	• No change in AV, IV. • Increasing of PV.	Sun, Yang, et al. (2023)
HMMT-1	Peanut	• Reducing the number of FAs. • No difference in the content of total tocopherols. • A slight decrease in the content of total sterol.	• Reduction of pigments in refined oil. • Reduction of PV.	Zhang et al. (2022)
0.45SDB -6-K-9@Fe_3O_4	Peanut	• Stability of FAs composition. • Reduction of V_E[p].	• No change in AV and MC. • Increasing trend of PV at different temperatures.	Ying et al. (2023)
Fe-BTC@Lac@FB	Peanut	• No significant change in FAs.	• No change in AV. • No leakage of Fe^{3+} in the oil content.	Rasheed, Ain, Ali, and Liu (2024)
0.2 % SAC	Peanut	• Maintain the content of phytosterols and tocopherols.	Not Reported	Jiang et al. (2023)
CS/SDS/AC	Peanut	• Slight decrease in total phenol content. • Retention of V_E and phytosterols. • Stability of volatile flavors.	Not Reported	(Ji et al., 2024)
Fe_3O_4@ATP	Peanut	• Stability of FAs composition. • Decrease in V_E and sterol contents.	Not Reported	Ji and Xie (2021)
MGO	Rice bran	● Stability of FAs and V_E.	• No change in AV and PV.	(Ji and Xie, 2019)
Cu-BTC MOF	Peanut Corn	• No change in FAs. • Stability of V_E. • Reduction of RV[q].	• No leakage of Cu in the oil content. • Lightning of oil color. • No change in AV and PV.	Ma et al. (2021)
FM@GO@Fe_3O_4	Corn Peanut	• Stability of FAs. • Reduction of RV and V_E.	• No change in oil color. • No leakage of Fe in the oil content. • No change in AV and PV.	(Ma et al., 2023)
VC-rGO/Fe_3O_4	Vegetable	• Reduction of sesamol, sesamin, and sesamolin from sesame oil. • No change in FAs.	• Reduction of pigments in refined oil. • Reduction of AV. • No change in PV.	Ma et al. (2024)
DC/CFOS NC	Vegetable	• No change in FAs and sterols.	• Increases in PV, AV, and *p*AV. • No leakage of Fe and Co. • Stability of MC and IV.	Abasi et al. (2023)
AC	Fig seed	• Reduction of phenolic content. • Reduction of antioxidant activity.	• Reduction of chlorophylls and carotenoids.	Senturk and Karaca (2022)
BF-NH_2-Lac	Corn	–	• No change in oil color. • No leakage of Cu^{2+} in the oil content. • Reducing of AV.	Rasheed, Ain, and Liu (2024)
MOF-235	Vegetable	• Stability of FAs composition. • Stability of phytosterols and V_E.	Not Reported	Du et al. (2023)
PL-GO_x- Fe_3O_4@COF	Vegetable	• Stability of phytosterols and V_E. • No significant change in FAs.	• No change in oil color. • No leakage of Fe in the oil content. • No change in AV, PV, and IV.	Fu et al. (2024)
Alkali-refining	Peanut	• No change in unsaturated FAs.	• Reducing of AV. • Increasing of PV. • Destruction of natural pigments by alkali (lightning of oil color).	(Ji et al., 2015)
Aspergillus luchuensis YZ-1	Vegetable	• Stability of FAs composition.	• No change in oil color.	Zhang et al. (2024)
Lac NF-P	Peanut	• No significant change in FAs.	• No change in AV and PV. • Reducing of IV. • No change in oil color. • No leakage of Cu^{2+} in the oil content.	Lu et al. (2023)
Pd@PCN-222	Corn	–	• No change in AV and IV. • No leakage of Pd and Zr.	Wei et al. (2022)
Pd@CRH-400	Corn	• Stability of FAs composition.	• No leakage of Pd in the oil content. • Stability of MC and IV. • Slight changes in AV, PV, and *p*-AV.	Zabeti et al. (2024)

[a] Fatty acid.
[b] Arachidic acid.
[c] Palmitic acid.
[d] Myristic acid.
[e] Stearic acid.

[f] Linoleic acid.
[g] Oleic acid.
[h] Linolenic acid.
[i] Acid value.
[j] Peroxide value.
[k] Saponification value.
[l] Moisture content.
[m] Refractive index.
[n] Iodine value.
[o] *Para*-Anisidine value.
[p] Vitamin E.
[q] Resveratrol value.

cultures (Lu et al., 2023). This study was accompanied by reactions including demethylation, decarbonylation, hydroxylation, and hydration, which reduced toxicity of all intermediate species. Demethylation and lactone ring opening played a role in these reactions. It is also worth mentioning that laccases, the enzymes most studied for detoxifying AFB1 in oily matrices, destroy AFB1 in two ways. At first, laccase reacts with the double bond in the end furan ring and thus causes the formation of AFB1-8-9-epoxide, which is much more toxic than the original substance (**BP1**). Therefore, to reduce toxicity, it becomes AFB1-8-9-dihydrodiol (**BP2**). In the second path laccase pathway, the addition of hydroxyl groups at carbon positions 10 and 11 directly leads to the opening of the lactone ring in AFB1 (**BP5**) (Rasheed, Ain, & Liu, 2024; Zhang et al., 2024).

4.4. Nanozyme peroxidase mechanism

No hazardous byproducts have been observed in nanozyme-based methods, particularly peroxidase nanozymes that rely on redox cycles followed by electron transfer to generate ROS. Based on the corresponding mechanisms and observed degradation pathways, it is evident that the cyclopentanone site is attacked and degraded by ROS (**NP1-NP3**). Electron transfer occurs much less frequently in other methods, indicating the high potential of this approach in degrading AFB1 (Faraji et al., 2023; Zhang et al., 2022). Additionally, the attack of ROS on sites such as the double bond and lactone ring in one pathway leads to the breaking of the double bond and the opening of the furan and lactone rings, accompanied by hydroxylation (**NP4-NP9**) (Wei et al., 2022). In another pathway, through processes such as dehydrogenation, dehydroxylation, and demethylation, products **NP10-NP14** are generated (Zhou et al., 2024). As shown in Table 4, $^{\bullet}OH$ produced in Fe_3O_4/-GO/NH_2-MIL-53(Fe)/H_2O_2 system could be oxidized the terminal furan ring, resulting in the formation of the product **NP15** (Wang et al., 2025). The cleavage of a carbonyl group from the cyclopentanone leads to the formation of **NP16**. In an alternative route, further removal of a carbonyl group from cyclopentanone, accompanied by the addition of two hydrogen atoms to C=C and subsequent decomposition of the lactone and furan structures through the elimination of C=O, CH, and CH_2 groups, yields the products **NP17** and **NP18**, respectively. In the next step, degradation of the O-CH_3 group attached to the benzene ring, breaking of the double bond in the terminal furan ring, and addition of a hydroxy group result in the formation of **NP19**. Finally, decomposition of the furan and lactone rings leads to the formation of **NP20**.

As previously mentioned, the chemical structure of AFB1, due to the presence of functional groups such as methoxy, lactone, cyclopentanone, and the double bond in the terminal furan ring, results in severe toxicity, carcinogenicity, and mutagenicity. Therefore, modifying these active sites may reduce this compound's toxicity and biological activity. According to the results of a study that led to the formation of intermediates **NP15**–**NP20**, and based on predictions made using the *T.E.S.T* software in the same study, the predicted oral LD_{50} of AFB1 in rats was estimated to be 11.50 mg kg^{-1}. This factor was predicted for products **NP17**, **NP19**, and **NP20** to be 130.12, 22.57, and 3347.67 mg kg^{-1}, respectively, clearly indicating a decrease in toxicity in these compounds (Wang et al., 2025). Since the lactone moiety and the double bond in the terminal furan ring (the primary sites for complex generation with proteins and nucleic acids in living organisms) are extensively and effectively responsible for toxicity, products **NP4**–**NP6**, **NP15**, and **NP16**, which underwent modifications or degradation in these sites, showed a significant reduction in toxicity.

Furthermore, it can be predicted using the mentioned software that the theoretical LD_{50} of product **NP18**, which results from further degradation of **NP17**, would be higher than that of AFB1, indicating lower toxicity (Liu, Li, Liu, & Bian, 2019; Wang et al., 2025). Additionally, since the fluorescence of AFB1 arises from specific structural features, particularly the lactone ring and the double bond in the terminal furan ring, any reduction or loss of fluorescence indicates molecular structural changes directly associated with decreased toxicity. In this context, Lee and colleagues observed a loss of fluorescence in the structures of **NP10** and **NP11**, attributed to the degradation of the lactone ring. They concluded that their toxicity was also reduced compared to the parent compound. According to the findings, other products that underwent modifications or degradation in the sites, as mentioned above, were also associated with reduced toxicity (Lee et al., 1981; Mao et al., 2016).

5. Comparison of AFB1-remediation technologies from oily matrices

A comparative analysis of prior state-of-the-art technologies and their merits/demerits is conducted to understand better the enzymatic-like efficiency in removing AFB1 from oil matrices. Primarily, the detailed evaluation of the "*SCUFEERS*" concept (*i.e., Safety, Capacity, Universality, Finance, Ecology, Efficiency, Rapidity, and Selectivity*) for detoxifying AFB1 from various edible oils was also performed (see Fig. 3).

5.1. Physical approaches

Physical methods such as irradiation, heat treatment, and photocatalysts have the potential to degrade/alter the chemical composition of the AFB1. Non-thermal processes, including those based on photocatalysts and irradiation methods such as UV light, have emerged as suitable alternatives to traditional thermal techniques for removing AFB1 from edible oils due to reduced energy consumption and lower CO_2 emissions. However, these methods may produce compounds with potentially toxic/hazardous effects on consumer health, which conflict with safety standards (Kolarič et al., 2024; Peng et al., 2023). On the other hand, due to the availability and readiness of technology/equipment and relatively high efficiency (80.0 %–100 %), these methods align well with the criteria of effectiveness and capacity. Despite high efficiency (77.3 %–99.4 %) and adsorption capacity of TiO_2 to hydrophilic AFB1, some factors (*e.g.,* the incompetent exploitation of UV–vis, non-uniform distribution in oily matrices, and recoverability of the TiO_2 nanoparticles after edible oil treatment) are limited the applicability of TiO_2-edible oil system (Table 1).

Additionally, concerning the selectivity criterion, it can be stated

that physical methods may significantly impact nutritional value and organoleptic profiles due to the production of intermediates and byproducts with varying toxicity. It is also worth noting that intense and prolonged irradiation may degrade the quality of food samples. Therefore, these methods do not align well with this criterion (Guo et al., 2021; Moradian et al., 2024).

Degradation of AFB1 from oil matrices by Plasma-based methods has not yet been reported. Challenges include the inactivity of plasma-generated species, lipid oxidation leading to peroxides or undesirable compounds, differences in electrical conductivity, electrical instability, and issues in plasma distribution within oil environments. Additionally, the high viscosity of oils, acting as a physical barrier that prevents active species and plasma gases such as O_2 or N_2 from reaching AFB1, further reduces effectiveness. Developing hybrid systems and optimizing gas

Table 4
Comparing the mechanisms and nature of produced intermediates in the degradation of AFB1 from oily matrices through various processes.

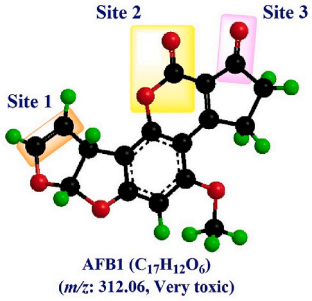

Method (Reference)	Transformed products
Physical (Song et al., 2024; Guo et al., 2021; Li et al., 2022; Pankaj, Shi, & Keener, 2018; Rushing & Selim, 2019; Peng et al., 2023; Liu et al., 2011; An et al., 2024; Xu et al., 2019; Liu et al., 2019; Nazhand et al., 2020; Shi, 2016; Zhang et al., 2018; Ma et al., 2021; Sun et al., 2021; Zhang et al., 2021b; Qi et al., 2023; Wang et al., 2022; Wang et al., 2011; Wang et al., 2020; Sun et al., 2023; Meng et al., 2024; Castro-Ríos et al., 2021)	**Path A** **PP1** ($C_{15}H_{10}O_5$) (*m/z*: 270.05, Less toxic) → **PP2** ($C_{15}H_{10}O_7$) (*m/z*: 302.14, More toxic) **Path B** **PP3** ($C_{17}H_{14}O_5$) (*m/z*: 298.08, Less toxic) → **PP4** ($C_{14}H_{12}O_5$) (*m/z*: 260.07, Less toxic) → **PP5** ($C_{14}H_{16}O_4$) (*m/z*: 248.10, Less toxic) → **PP6** ($C_{11}H_{10}O_2$) (*m/z*: 174.07, Very low toxicity) **Path C** **PP7** ($C_{16}H_{12}O_6$) (*m/z*: 300.06, Less toxic) → **PP8** ($C_{17}H_{14}O_6$) (*m/z*: 314.08, Less toxic) → **PP9** ($C_{14}H_{10}O_6$) (*m/z*: 274.05, Less toxic) **Path D** **PP10** ($C_{17}H_{14}O_8$) (*m/z*: 346.07, More toxic) → **PP11** ($C_{14}H_{12}O_5$) (*m/z*: 260.07, Less toxic) → **PP12** ($C_{14}H_{10}O_6$) (*m/z*: 274.05, Less toxic) **Path E** **PP13** ($C_{17}H_{14}O_7$) (*m/z*: 330.07, Less toxic) → **PP14** ($C_{16}H_{14}O_6$) (*m/z*: 302.08, Less toxic) → **PP15** ($C_{17}H_{14}O_7$) (*m/z*: 330.07, Less toxic) **Path F** **PP16** ($C_{17}H_{14}O_8$) (*m/z*: 346.07, Less toxic) → **PP17** ($C_{16}H_{16}O_6$) (*m/z*: 304.09, Non-toxic)

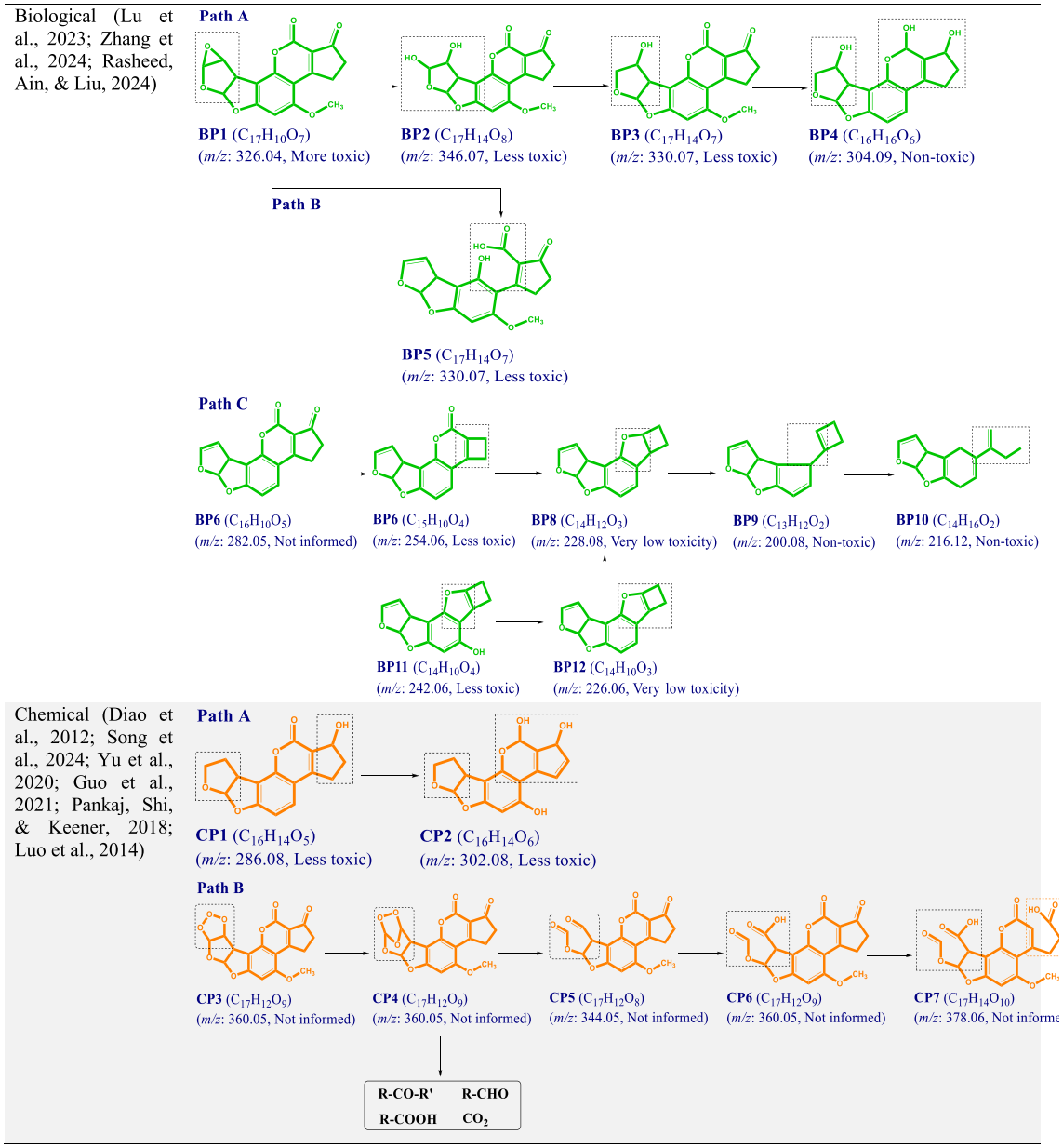
Biological (Lu et al., 2023; Zhang et al., 2024; Rasheed, Ain, & Liu, 2024)
Path A
BP1 (C17H10O7)
(m/z: 326.04, More toxic)
BP2 (C17H14O8)
(m/z: 346.07, Less toxic)
BP3 (C17H14O7)
(m/z: 330.07, Less toxic)
BP4 (C16H16O6)
(m/z: 304.09, Non-toxic)
Path B
BP5 (C17H14O7)
(m/z: 330.07, Less toxic)
Path C
BP6 (C16H10O5)
(m/z: 282.05, Not informed)
BP6 (C15H10O4)
(m/z: 254.06, Less toxic)
BP8 (C14H12O3)
(m/z: 228.08, Very low toxicity)
BP9 (C13H12O2)
(m/z: 200.08, Non-toxic)
BP10 (C14H16O2)
(m/z: 216.12, Non-toxic)
BP11 (C14H10O4)
(m/z: 242.06, Less toxic)
BP12 (C14H10O3)
(m/z: 226.06, Very low toxicity)
Chemical (Diao et al., 2012; Song et al., 2024; Yu et al., 2020; Guo et al., 2021; Pankaj, Shi, & Keener, 2018; Luo et al., 2014)
Path A
CP1 (C16H14O5)
(m/z: 286.08, Less toxic)
CP2 (C16H14O6)
(m/z: 302.08, Less toxic)
Path B
CP3 (C17H12O9)
(m/z: 360.05, Not informed)
CP4 (C17H12O9)
(m/z: 360.05, Not informed)
CP5 (C17H12O8)
(m/z: 344.05, Not informed)
CP6 (C17H12O9)
(m/z: 360.05, Not informed)
CP7 (C17H14O10)
(m/z: 378.06, Not informe
R-CO-R'
R-CHO
R-COOH
CO2

	Path C 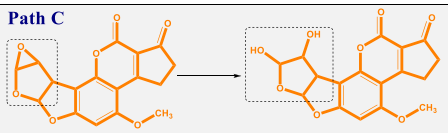 **CP8** ($C_{17}H_{12}O_7$) (*m/z*: 328.06, More toxic) **CP9** ($C_{17}H_{14}O_8$) (*m/z*: 346.07, Less toxic) **Path D** 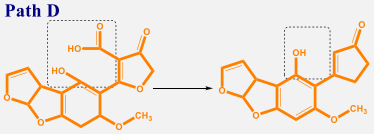 **CP10** ($C_{16}H_{14}O_8$) (*m/z*: 334.07, Less toxic) **CP11** ($C_{16}H_{14}O_5$) (*m/z*: 286.08, Less toxic) **Path E** 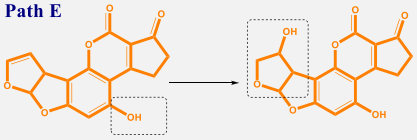 **CP12** ($C_{16}H_{10}O_6$) (*m/z*: 298.05, Less toxic) **CP13** ($C_{16}H_{12}O_7$) (*m/z*: 316.06, Less toxic)
Nanozyme peroxidase (Wei et al., 2022; Zabeti et al., 2024; Zhou et al., 2024; Faraji et al., 2023; Zhang et al., 2022; Wang et al., 2025)	**Path A** 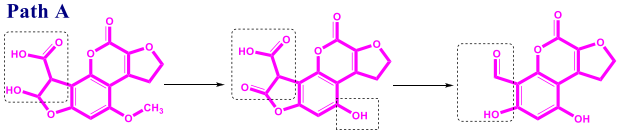 **NP1** ($C_{15}H_{12}O_8$) (*m/z*: 320.05, Less toxic) **NP2** ($C_{14}H_8O_8$) (*m/z*: 304.02, Less toxic) **NP3** ($C_{12}H_8O_6$) (*m/z*: 248.03, Less toxic) **Path B** 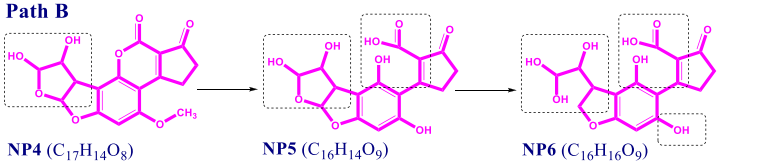 **NP4** ($C_{17}H_{14}O_8$) (*m/z*: 346.07, Less toxic) **NP5** ($C_{16}H_{14}O_9$) (*m/z*: 350.06, Less toxic) **NP6** ($C_{16}H_{16}O_9$) (*m/z*: 352.08, Very low toxicity) **Path C** 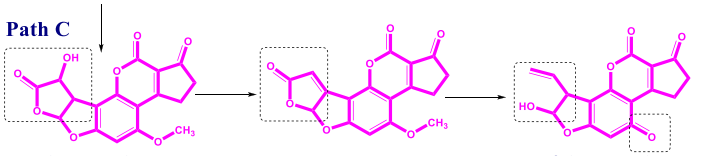 **NP7** ($C_{17}H_{12}O_8$) (*m/z*: 344.05, Less toxic) **NP8** ($C_{17}H_{10}O_7$) (*m/z*: 326.04, Less toxic) **NP9** ($C_{16}H_{11}O_6$) (*m/z*: 299.06, Less toxic)

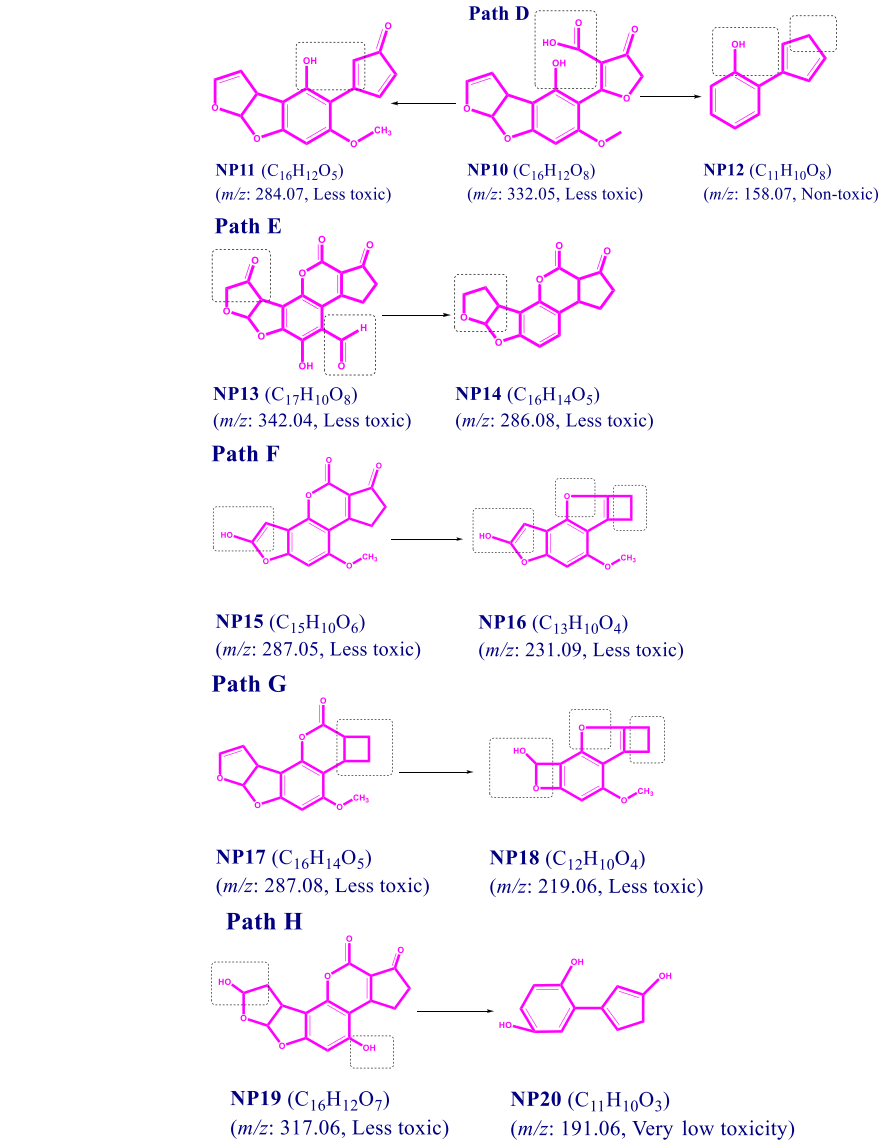

input to enhance active species production could improve the efficacy of cold plasma technology in oil matrices.

5.2. Chemical approaches

Chemical methods rely on chemical reactions such as decomposition, substitution, oxidation-reduction, and hydrolysis in liquid, solid, and gaseous environments to AFB1 degrade/deactivate from oily matrices. The ozonation, intense oxidation process, and EOW are typically associated with reactant changes and the production of secondary pollution compounds (Kolarič et al., 2024). Consequently, the *Codex* Alimentarius standards and *European* regulations consider using the residues of chemical reagents, solvents, and oxidation byproducts inconsistent with public health standards (Peng et al., 2018; Shanakhat et al., 2018). It is essential to optimize chemical technologies to minimize AFB1 while preserving the highest quality of the oil (*e.g.,* FFAs, PV, AV, IV, and the overall phytosterols content in oils). As Zhu et al. (2016) indicated, the chemical methods significantly decreased the amounts of total tocols (9.50 %), total phytosterols (23.0 %), and squalene (24.0 %). Therefore, applying chemical processes is deemed non-compliant with safety standards. Additionally, the low efficiency at a long time (*e.g.,* 89.4 % at 60.0 h in ozonation process), ineffective mineralization, high energy consumption, need for harsh conditions (*e.g.,* T > 43.5 °C and high dose of alkaline reagent in alkali-remediation process, and high pH value (>12.0) in alkaline electrolyzed water process), the generation of waste products such as carbon dioxide, and limitations in actual application/implementation are restricted these methods (Table 1) (Ismail et al., 2018). This aspect also conflicts with environmental standards, particularly sustainability principles and green initiatives (Kolarič et al., 2024). Thus, chemical methods are not sufficiently specific and do not adequately meet the selectivity criterion, as they may produce compounds with relatively toxic effects on nutritional value, technological quality, and organoleptic profiles. Consequently, chemical methods are deemed insufficiently qualified for the AFB1 degradation from oily matrices (Ismail et al., 2018; Pankaj et al., 2018).

5.3. Biological approaches

Biological processes generally occur through enzymatic reactions or microbial metabolic activities within a cell or liquid environment. The

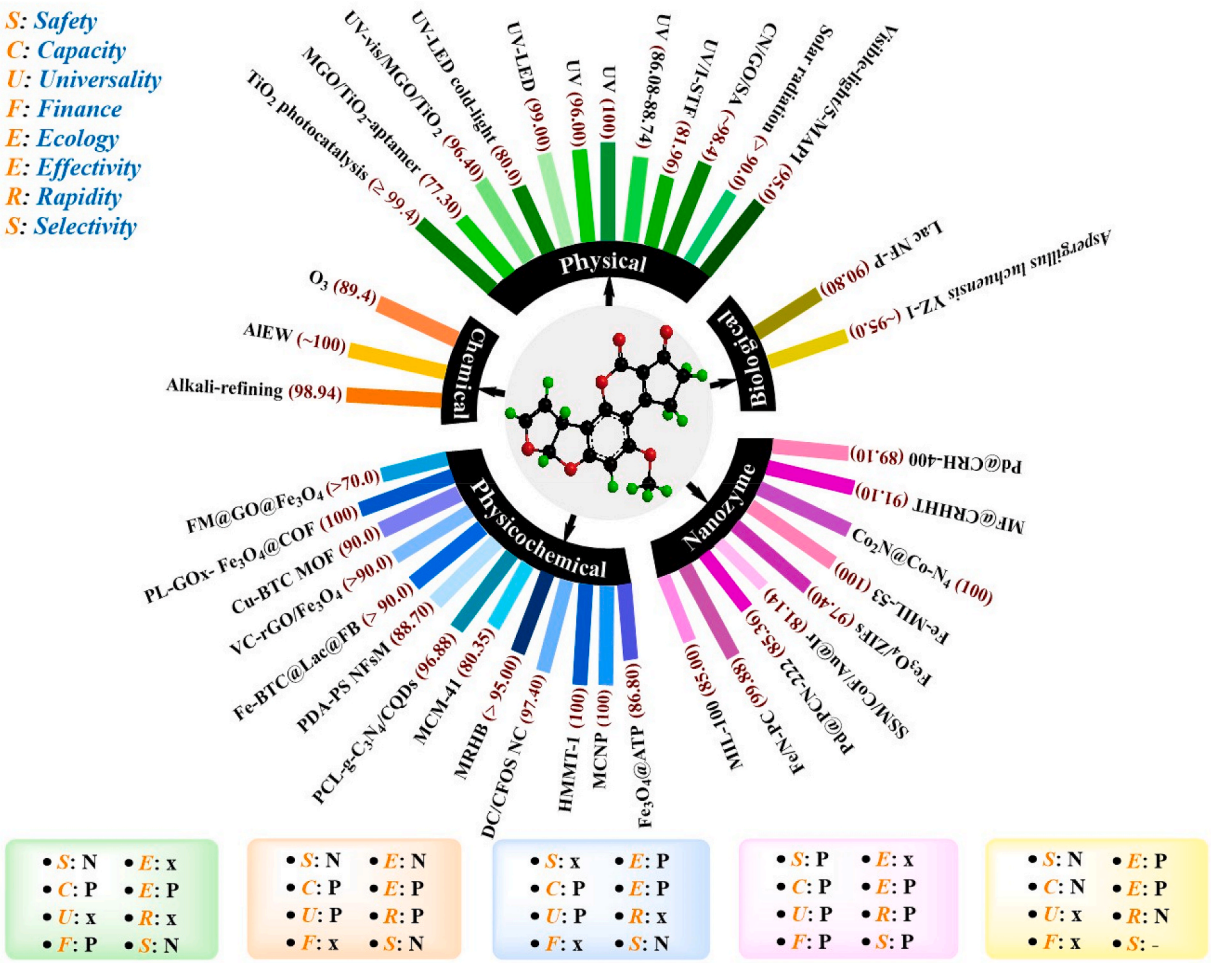

Fig. 3. Comparison of methods used in AFB1 removal from edible oils [**N**: Negative effect; **P**: Without adverse effect; **x**: Neutral effect].

substrate undergoes biochemical transformations in these methods to produce other chemical compounds (An et al., 2024). In biological processes, selectivity can be somewhat enhanced by utilizing specific enzymes or a consortium of microorganisms. However, inevitable hazardous byproducts with relatively high toxicity and sludge formation may occur, potentially reducing food quality/taste and making them incompatible with safety standards (Kolarič et al., 2024). Due to their low energy consumption and environmentally friendly nature, biological technologies align well with ecological standards.

Nevertheless, because of the complexity of scaling up these processes for industrial applications and their time-consuming nature, they fail to meet the criteria of capacity and speed (Da silva et al., 2018). Biological methods have minimal applications in oily matrices due to the low activity of many enzymes/microorganisms in such environments. As a dense matrix, the oil can inhibit the transfer of nutrients or oxygen, thereby restricting biological activity.

5.4. Physicochemical approaches

Physicochemical processes involve precise interactions between AFB1 and an appropriate adsorption matrix, forming a complex matrix through intermolecular forces (Song et al., 2024). Since the matrices used in adsorption processes are of natural origin (*e.g.,* rice husk waste, chitosan, biochar, etc.), and these methods do not produce hazardous byproducts, they do not significantly reduce the quality or value of foods after treatment (Moradian et al., 2024). On the other hand, due to their low selectivity, adsorbents not only adsorb AFB1 but also absorb different nutrients, vitamins, and mineral compounds. Moreover, implementing such processes does not require expensive equipment or high energy consumption, aligning with financial and ecological criteria (Kolarič et al., 2024; Abbasi et al., 2023).

5.5. Enzymatic-like approaches

Nanozyme activity mainly depends on the active center size and dispersion quality. At the same time, the stable polydispersity of metal nanoparticles is remarkably related to powerful metal-support interactions and the chemistry of support (*i.e.,* chemical composition, surface morphology, porosity, surface area, and lipophilicity). Thus, to achieve food safety in a nanozyme-based system, nanozymes are constructed from green and inexpensive support with strong metal-support interactions to prevent the loss of toxic metal nanoparticles. For example, Zabeti et al. and Zhang et al. used rice husk and porous carbon as green and favorable supports to fabricate robust nanozymes with low leaching rates of toxic metals to reaction matrices, respectively, which confirmed by ICP-OES analysis and recovery test (Zabeti et al., 2024; Zhang et al., 2022). Based on the ICP-OES results, a trace amount of Pd (0.0187 mg L^{-1}) ions were released to matrices after seven peroxidase-like cycles, which proved the high structural/chemical stability of Pd@CRH-400 with a low level of heavy metals leaching (Zabeti et al., 2024).

From a cost-effective point of view, various nanozyme such as Pd@CRH-400, Fe_3O_4/GO/NH_2-MIL-53(Fe), Pd@PCN-222, SSM/COF/Au@Ir, MF@CRHHT, and MOFs embedded in polymeric membranes have provided clear evidence of their high-performance, structural stability, recoverability, and potential for cost-effective production. The

synthesis methods for these nanozymes are generally based on simple and accessible techniques such as wet chemical synthesis, co-precipitation, bio-based pyrolysis, or hydrothermal synthesis. These approaches do not require advanced equipment and are readily scalable. The use of natural and low-cost raw materials, such as rice husk, chitosan, and common metal precursors, has contributed to the overall cost-effectiveness of these systems concerning their high catalytic efficiency. For instance, Fe_3O_4 nanozyme could be synthesized via a simple co-precipitation method at approximately $70 per gram, whereas high-purity horseradish peroxidase costs over $400 per gram (Gao et al., 2007). Regarding stability, nanozymes could retain activity across a 20–90 °C temperature range and a pH range of 3.0–10.0.

In contrast, natural enzymes typically denature at high temperatures and have a limited functional pH range. Moreover, nanozymes can be recovered efficiently in consecutive cycles, while natural enzymes are used only in one or at most two cycles (Zabeti et al., 2024; Faraji et al., 2023; Huang, Ren, and Qu, 2019). Additionally, Pd@CRH-400 may initially appear more expensive than traditional adsorbents due to the incorporation of noble metals like palladium and specific nanostructure. However, their exceptionally high removal efficiency, reusability over multiple consecutive cycles (at least seven cycles) with a removal rate of 96.1 %, and excellent structural and chemical stability lead to reduced operational costs and less frequent replacement over time, offsetting the initial expenses. The leaching of Pd into the aqueous medium after seven cycles was reported to be only 0.0187 mg L^{-1}, which is negligible from an environmental standpoint (Zabeti et al., 2024). Similarly, the Fe_3O_4/GO/NH_2-MIL-53(Fe) nanozyme synthesized using readily available and low-cost raw materials such as graphene oxide, iron nanoparticles, and MIL-53(Fe) through a simple hydrothermal method has demonstrated remarkable performance in terms of structural stability, reusability, and economic efficiency for industrial applications (Wang et al., 2025). The results of TGA and XRD analyses before and after the synergistic adsorption and degradation processes of AFB1 indicate the nanozyme's good thermal resistance (with only an 8.16 % weight loss observed in the sample) and retention of its original crystalline structure. The concentration of Fe ions released to the medium after the reaction was only 0.003 mg L^{-1}, which is significantly below the typical detection limit, reflecting the high chemical stability of the nanozyme. In terms of recovery and reuse, the nanozyme was easily separated using an external magnetic field, owing to the magnetic property of the Fe_3O_4 core, and was successfully reused for up to eight consecutive cycles without significant performance loss, maintaining an efficiency above 90.0 %. This demonstrates the high catalytic performance, stability, and cost-benefit of the nanozymes during repeated applications.

As well as, Pd@PCN-222 demonstrated sustained performance over five cycles, maintaining removal efficiencies above 91 % with minimal decline (Wei et al., 2022). In the case of systems such as SSM/CO-F/Au@Ir or MF@CRHHT, the integration of peroxidase-like nanozymes led to rapid and efficient degradation of AFB1. These systems were designed with high surface activity, uniform metal dispersion, and good substrate accessibility. Although they may appear costly due to more advanced components, their multifunctionality (*e.g.,* simultaneous adsorption and catalytic degradation) significantly lowers the overall cost in practical applications (Faraji et al., 2023; Zhou et al., 2024).

Additionally, in polymeric membranes embedded with enzyme-like MOFs, the design supports a multifunctional and regenerable platform with potential recovery during or after adsorption-degradation. Given the ability to be reused in multiple cycles, sustained high performance, and ease of synthesis without reliance on advanced instrumentation, these nanozymes can be considered economically favorable alternatives to conventional adsorbents. While initial production costs may be higher in some cases, the durability and reusability of these materials contribute to long-term cost savings (Ren et al., 2019). Therefore, from both technical and economic perspectives, the proposed nanozyme systems are competitive with conventional adsorbents and superior in many real-world applications.

Besides, H_2O_2 and nanozyme dosages should be in the appropriate ratio (optimal dosages) to achieve minimal damage to edible oils' organoleptic/physicochemical properties. At higher concentrations (>4.0 mM) or prolonged treatment times, H_2O_2 plays a significant role in altering oil quality indices (*e.g.,* the increase in peroxide value and anisidine value), indicating enhanced lipid oxidation (Shen and Singh, 2021; Zabeti et al., 2024). Moreover, the degradation of essential fatty acids and the reduction of antioxidant compounds are other adverse effects contributing to the decline in oil quality. Thus, using H_2O_2 under optimum amounts and controlled operational conditions in processes does not cause significant side effects.

On the other hand, through oxidative degradation processes, these nanozymes convert AFB1 into non-toxic or less toxic compounds by destroying bifuran/lactone rings as major toxic sites of AFB1, demethylation, hydroxylation, etc. Studies have shown that the toxicity of produced intermediates is significantly lower than that of other techniques (Demkiv et al., 2021). Therefore, due to the lack of hazardous metals/byproducts in reaction matrices and no adverse effects on taste, color, or nutritional value of oils attributable to the high selectivity of nanozymes they align well with the primary criterion of ensuring food safety and quality (Ren et al., 2019). In addition to their lower production costs, peroxidase nanozymes, owing to their high active surface area, also enhance the rate and efficiency of AFB1 removal, making them compatible with finance, efficiency, and rapidity criteria.

Furthermore, their stability under various conditions enables them to remove AFB1 at a wide range of pH and temperatures over repeated cycles, demonstrating their alignment with the capacity criterion (Wei et al., 2022). Finally, based on the provided information comparing and evaluating methods for AFB1 degradation and removal, it appears that processes based on peroxidase nanozymes generally have the most significant potential for application in oil matrices, which is primarily attributed to their strong alignment with the "*SCUFEERS*" criteria.

6. Conclusions and future research necessities

Since AFB1 has a lipophilic structure, it exhibits high stability in nonpolar oil matrices, significantly enhancing the toxicity of edible oils (*e.g.,* peanut, sesame, groundnut, coconut, and olive oils). Considering the importance of edible oils in providing calories, essential fatty acids, vitamins, phytosterols, and 30 % of the daily human diet, the need to remove AFB1 using advanced technologies has become increasingly important. This paper aims to comprehensively review the prevalence/distribution of AFB1 in various edible oils, mainly focusing on peroxidase nanozyme-based processes as a novel approach along with merits/demerits and challenges, mechanisms, the toxicity of intermediate/byproducts, and comparison with other methods. This presentation follows briefly the following results.

- Nanozymes and hydrogen peroxide mimic enzymatic activity to generate ROS that detoxify AFB1. Comparatively, nanozymes are high-entropy nanomaterials with high and tunable catalytic activity and stability, high recycling capability related to the heterogeneity and magnetic property, controllable enzymatic-like activity via experimental parameters (*e.g.,* temperature, H_2O_2 dosage, pH, etc.) and physicochemical properties (*e.g.,* shape, size, surface lipophilicity/hydrophilicity, chemical structure and composition), which can degrade AFB1 into simple, non-toxic compounds while preserving food products' nutritional value and quality. Despite their remarkable merits, a few shortcomings (*e.g.,* limited types, substrate selectivity of nanozyme, and potential nano-toxicity) still need to be addressed before large-scale commercial application.
- For designing new kind of versatile nanozymes, the structure-activity relationship, using a cost-effective, green, non-toxic, and biodegradable capping/stabilizing agent, and multi-metallicity with metal-metal interactivity for the improved catalytic activity should be significantly considered. Besides, the optimization of peroxidase-

nanozymes should be based on imitating natural enzyme structures (*i.e.,* geometry and oxidation state of the metal center, the surrounding environment of ligands, hydrophilicity/hydrophobicity, and substrate selectivity).

- More importantly, no/little leaching of toxic heavy metal ions from nanozyme surface into the food matrix below the maximum acceptable level of toxic metals is one of the significant challenges. To resist the deactivation of peroxidase activity and control food safety, nanozyme should be stable towards metallic active sites leaching into the food matrix under operating conditions. Metal poisoning of peroxidase-treated oily matrices could be minimized by boosting the long-term stability of nanozyme and using less toxic alternatives to harmful metals.
- Compared to single-metal nanozymes, electron-rich multi-metallic nanozymes, exhibit enhanced catalytic performance owing to high electron transfer between constituent metals, favorable metal–support synergism, and affirmative change in the oxygen vacancies or phase properties. However, the inherent thermodynamic instability of multi-metallic-based nanomaterials is a challenging problem and a future trend.
- Compared to aqueous matrices, the nonpolar nature of oils, low stability of active radicals, and reduced dispersion are the main reasons for the lower efficiency of peroxidase nanomaterials in detoxifying AFB1 from oil matrices. However, advanced techniques such as encapsulating nanozymes, modifying the surface of nanozymes with hydrophobic ligands, using emulsion systems, or adding surfactants to improve the dispersion of nanozymes and hydrogen peroxide in oil matrices can significantly overcome these limitations and improve their performance and efficiency in the future.

It is hoped that this study will enable researchers to focus on designing, fabricating, implementing, and delivering the best processes with the highest potential and minimal invasiveness by utilizing the mentioned criteria. It also aims to understand peroxidase nanozyme-based methods better, which have attracted significant attention due to their strong alignment with the *SCUFEERS* framework criteria.

Declaration of competing interest

No conflict to declare.

Acknowledgment

A.F. acknowledges the research council of Tehran Medical Sciences, Islamic Azad University, for the research founding of this project. Open access funding provided by Universidad Pública de Navarra.

Data availability

No data was used for the research described in the article.

References

Abasi, N., Faraji, A. R., & Davood, A. (2023). Adsorptive removal of aflatoxin B 1 from water and edible oil by dopamine-grafted biomass chitosan–iron–cobalt spinel oxide nanocomposite: Mechanism, kinetics, equilibrium, thermodynamics, and oil quality. *RSC Advances, 13*(49), 34739–34754. .

Abrehame, S., Manoj, V. R., Hailu, M., Chen, Y. Y., Lin, Y. C., & Chen, Y. P. (2023). Aflatoxins: Source, detection, clinical features and prevention. *Processes, 11*(1), 204.

An, N. N., Shang, N., Zhao, X., Tie, X. Y., Guo, W. B., Li, D., … Wang, Y. (2024). Occurrence, regulation, and emerging detoxification techniques of aflatoxins in maize: A review. *Food Reviews International, 40*(1), 92–114.

Aringbangba, O. E., Oluwafemi, F., Kolapo, A. L., Adeogun, A. I., & Popoola, T. O. (2021). Elimination of aflatoxins from two selected Nigerian vegetable oils using magnetic chitosan nanoparticles. *Industria: Jurnal Teknologi dan Manajemen Agroindustri, 10*(1), 1–11.

Bilgrami, K. S., & Sinha, K. K. (2024). Aflatoxins: Their biological effects and ecological significance. In *Handbook of applied mycology* (pp. 59–86). CRC Press.

Bordin, K., Sawada, M. M., Rodrigues, C. E. D. C., da Fonseca, C. R., & Oliveira, C. A. F. (2014). Incidence of aflatoxins in oil seeds and possible transfer to oil: A review. *Food Engineering Reviews, 6*, 20–28.

Castro-Ríos, K., Montoya-Estrada, C. N., Martínez-Miranda, M. M., Hurtado Cortés, S., & Taborda-Ocampo, G. (2021). Physicochemical treatments for the reduction of aflatoxins and *Aspergillus niger* in corn grains (*Zea mays*). *Journal of the Science of Food and Agriculture, 101*(9), 3707–3713.

Cavaliere, C., Foglia, P., Guarino, C., Nazzari, M., Samperi, R., & Laganà, A. (2007). Determination of aflatoxins in olive oil by liquid chromatography–tandem mass spectrometry. *Analytica Chimica Acta, 596*(1), 141–148.

Chen, R., Ma, F., Li, P. W., Zhang, W., Ding, X. X., Zhang, Q. I., & Xu, B. C. (2014). Effect of ozone on aflatoxins detoxification and nutritional quality of peanuts. *Food Chemistry, 146*, 284–288. .

Chen, L., Molla, A. E., Getu, K. M., Ma, A., & Wan, C. (2019). Determination of aflatoxins in edible oils from China and Ethiopia using immunoaffinity column and HPLC-MS/MS. *Journal of AOAC International, 102*(1), 149–155.

Da silva, E., Bracarense, A., & Oswald, I. (2018). Mycotoxins and oxidative stress: Where are we? *World Mycotoxin Journal, 11*(1), 113–134.

Dai, H., Liang, S., Shan, D., Zhang, Q., Li, J., Xu, Q., & Wang, C. (2022). Efficient and simple simultaneous adsorption removal of multiple aflatoxins from various liquid foods. *Food Chemistry, 380*, Article 132176.

Dai, C., Sharma, G., Liu, G., Shen, J., Shao, B., & Hao, Z. (2024). Therapeutic detoxification of quercetin for aflatoxin B1-related toxicity: Roles of oxidative stress, inflammation, and metabolic enzymes. *Environmental Pollution*, Article 123474.

Demkiv, O., Stasyuk, N., Serkiz, R., Gayda, G., Nisnevitch, M., & Gonchar, M. (2021). Peroxidase-like metal-based nanozymes: Synthesis, catalytic properties, and analytical application. *Applied Sciences, 11*(2), 777.

Deng, H., Su, X., & Wang, H. (2018). Simultaneous determination of aflatoxin B1, bisphenol A, and 4-nonylphenol in peanut oils by liquid-liquid extraction combined with solid-phase extraction and ultra-high performance liquid chromatography-tandem mass spectrometry. *Food Analytical Methods, 11*, 1303–1311.

Dey, C., Kundu, T., Biswal, B. P., Mallick, A., & Banerjee, R. (2014). Crystalline metal-organic frameworks (MOFs): Synthesis, structure and function. *Acta Crystallographica Section B: Structural Science, Crystal Engineering and Materials, 70*(1), 3–10.

Diao, E., Shan, C., Hou, H., Wang, S., Li, M., & Dong, H. (2012). Structures of the ozonolysis products and ozonolysis pathway of aflatoxin B1 in acetonitrile solution. *Journal of Agricultural and Food Chemistry, 60*(36), 9364–9370.

Diao, E., Shen, X., Zhang, Z., Ji, N., Ma, W., & Dong, H. (2015). Safety evaluation of aflatoxin B1 in peanut oil after ultraviolet irradiation detoxification in a photodegradation reactor. *International Journal of Food Science and Technology, 50*(1), 41–47.

Du, Q., Zhang, W., Xu, N., Jiang, X., Cheng, J., Wang, R., & Wang, P. (2023). Efficient and simultaneous removal of aflatoxin B1, B2, G1, G2, and zearalenone from vegetable oil by use of a metal–organic framework absorbent. *Food Chemistry, 418*, Article 135881.

Einolghozati, M., Talebi-Ghane, E., Ranjbar, A., & Mehri, F. (2021). Concentration of aflatoxins in edible vegetable oils: A systematic meta-analysis review. *European Food Research and Technology, 247*(12), 2887–2897.

Fan, S., Zhang, F., Liu, S., Yu, C., Guan, D., & Pan, C. (2013). Removal of aflatoxin B1 in edible plant oils by oscillating treatment with alkaline electrolysed water. *Food Chemistry, 141*(3), 3118–3123.

Faraji, A. R., Khoramdareh, N. B., Falahati, F., Jafari, S., Monfared, S. A., & Faghih, A. (2023). Superparamagnetic MnFe alloy composite derived from cross-bindered of chitosan/rice husk waste/iron aluminate spinel hercynite for rapid catalytic detoxification of aflatoxin B1: Structure, performance and synergistic mechanism. *International Journal of Biological Macromolecules, 234*, Article 123709.

Francis, S., Kortei, N. K., Sackey, M., & Richard, S. A. (2024). Aflatoxin B1 induces infertility, fetal deformities, and potential therapies. *Open Medicine, 19*(1), Article 20240907.

Fu, C., Hou, L., Chen, D., Huang, T., Yin, S., Ding, P., … Li, X. (2024). Targeted detoxification of aflatoxin B1 in edible oil by an enzyme–metal nanoreactor. *Journal of Agricultural and Food Chemistry, 72*(11), 5966–5974.

Guo, J., Shi, F., Sun, M., Ma, F., & Li, Y. (2022). Antioxidant and aflatoxin B1 adsorption properties of Eucheuma cottonii insoluble dietary fiber. *Food Bioscience, 50*, Article 102043.

Guo, Y., Zhao, L., Ma, Q., & Ji, C. (2021). Novel strategies for degradation of aflatoxins in food and feed: A review. *Food Research International, 140*, Article 109878.

Hanigan, H. M., & Laishes, B. A. (1984). Toxicity of aflatoxin B1 in rat and mouse hepatocytes in vivo and in vitro. *Toxicology, 30*(3), 185–193.

Ismail, A., Gonçalves, B. L., de Neeff, D. V., Ponzilacqua, B., Coppa, C. F., Hintzsche, H., … Oliveira, C. A. (2018). Aflatoxin in foodstuffs: Occurrence and recent advances in decontamination. *Food Research International, 113*, 74–85.

Javanmardi, F., Khodaei, D., Sheidaei, Z., Bashiry, M., Nayebzadeh, K., Vasseghian, Y., & Mousavi Khaneghah, A. (2022). Decontamination of aflatoxins in edible oils: A comprehensive review. *Food Reviews International, 38*(7), 1410–1426.

Ji, N., Diao, E., Li, X., Zhang, Z., & Dong, H. (2016). Detoxification and safety evaluation of aflatoxin B1 in peanut oil using alkali refining. *Journal of the Science of Food and Agriculture, 96*(12), 4009–4014.

Ji, J., & Xie, W. (2020). Detoxification of Aflatoxin B1 by magnetic graphene composite adsorbents from contaminated oils. *The Journal of Hazardous Materials, 381*, Article 120915.

Ji, J., & Xie, W. (2021). Removal of aflatoxin B1 from contaminated peanut oils using magnetic attapulgite. *Food Chemistry, 339*, Article 128072.

Ji, J., Xu, F., Jiang, M., Li, C., & Li, N. (2025). Activated carbon co-modified by chitosan and SDS for targeted removal of aflatoxins from fragrant peanut oil. *Food Chemistry, 463*, Article 141479.

Jiang, M., Ji, J., Zhang, Y., & Sun, S. (2023). Removal of aflatoxins in peanut oils by activated carbon functionalized with sodium dodecyl sulfonate. *Food Control, 153*, Article 109935.
Jiang, D., Ni, D., Rosenkrans, Z. T., Huang, P., Yan, X., & Cai, W. (2019). Nanozyme: New horizons for responsive biomedical applications. *Chemical Society Reviews, 48*(14), 3683–3704.
Jubeen, F., Zahra, N., Nazli, Z. I. H., Saleemi, M. K., Aslam, F., Naz, I., … Iqbal, M. (2022). Risk assessment of hepatocellular carcinoma with aflatoxin B1 exposure in edible oils. *Toxins, 14*(8), 547.
Kamimura, H., Nishijima, M., Tabata, S., Yasuda, K., Ushiyama, H., & Nishima, T. (1986). Survey of mycotoxins contamination in edible oil and fate of mycotoxins during oil-refining processes. *Food hygiene and safety science (Shokuhin Eiseigaku Zasshi), 27*(1), 59–63_1.
Karunarathna, N. B., Fernando, C. J., Munasinghe, D. M. S., & Fernando, R. (2019). Occurrence of aflatoxins in edible vegetable oils in Sri Lanka. *Food Control, 101*, 97–103.
Kasun, B. T., & Vanniarachchy, M. P. G. (2023). Reduction of Aflatoxin contamination in coconut oil using concentrated solar radiation. *Food Chemistry Advances, 3*, Article 100513.
Khan, R., Anwar, F., & Ghazali, F. M. (2024). A comprehensive review of mycotoxins: Toxicology, detection, and effective mitigation approaches. *Heliyon*.
Kolarič, L., Minarovičová, L., Lauková, M., Kohajdová, Z., & Šimko, P. (2024). Elimination of aflatoxin M1 from milk: Current status, and potential outline of applicable mitigation procedures. *Trends in Food Science & Technology*, Article 104603.
Ku, M., Li, J., Zhang, W., Sun, S., Zhang, Y., & Xie, Y. (2024). Degradation of AFB1 in edible oil by aptamer-modified TiO2 composite photocatalytic materials: Selective efficiency, degradation mechanism and toxicity. *Food Chemistry*, Article 142674.
Lee, L. S., Dunn, J. J., DeLucca, A. J., & Ciegler, A. (1981). Role of lactone ring of aflatoxin B 1 in toxicity and mutagenicity. *Experientia, 37*, 16–17.
Li, C., Liu, X., Wu, J., Ji, X., & Xu, Q. (2022). Research progress in toxicological effects and mechanism of aflatoxin B1 toxin. *PeerJ, 10*, Article e13850.
Li, Y. N., Wang, R., Luo, X., Chen, Z., Wang, L., Zhou, Y., … Zhang, C. (2022). Synthesis of rice husk-based MCM-41 for removal of aflatoxin B1 from peanut oil. *Toxins, 14*(2), 87.
Li, P., Wang, S., Lv, B., Zhang, M., Xing, C., Sun, X., & Fang, Y. (2023). Magnetic rice husk-based biochar for removal of aflatoxin B1 from peanut oil. *Food Control, 152*, Article 109883.
Lin, X., Hu, X., Zhang, Y., Xia, Y., & Zhang, M. (2019). Bioaccessibility in daily diet and bioavailabilityin vitro of aflatoxins from maize after cooking. *World Mycotoxin Journal, 12*(2), 173–182.
Liu, R., Jin, Q., Huang, J., Liu, Y., Wang, X., Mao, W., & Wang, S. (2011). Photodegradation of aflatoxin B 1 in peanut oil. *European Food Research and Technology, 232*, 843–849.
Liu, Y., Li, M., Liu, Y., Bai, F., & Bian, K. (2019). Effects of pulsed ultrasound at 20 kHz on the sonochemical degradation of mycotoxins. *World Mycotoxin Journal, 12*(4), 357–366.
Liu, Y., Li, M., Liu, Y., & Bian, K. (2019). Structures of reaction products and degradation pathways of aflatoxin B1 by ultrasound treatment. *Toxins, 11*(9), 526.
Liu, Y., & Wu, F. (2010). Global burden of aflatoxin-induced hepatocellular carcinoma: A risk assessment. *Environmental Health Perspectives, 118*(6), 818–824.
Lu, T., Fu, C., Xiong, Y., Zeng, Z., Fan, Y., Dai, X., … Li, X. (2023). Biodegradation of aflatoxin B1 in peanut oil by an amphipathic laccase–inorganic hybrid nanoflower. *Journal of Agricultural and Food Chemistry, 71*(8), 3876–3884.
Luo, X., Wang, R., Wang, L., Li, Y., Bian, Y., & Chen, Z. (2014). Effect of ozone treatment on aflatoxin B1 and safety evaluation of ozonized corn. *Food Control, 37*, 171–176.
Ma, F., Cai, X., Mao, J., Yu, L., & Li, P. (2021). Adsorptive removal of aflatoxin B1 from vegetable oils via novel adsorbents derived from a metal-organic framework. *The Journal of Hazardous Materials, 412*, Article 125170.
Ma, F., Tang, F., Yang, B., Guo, Q., Li, P., & Yu, L. (2024). Vitamin C-reduced graphene oxide/Fe_3O_4 composite for simultaneous removal of aflatoxin B1 and benzo (a) pyrene in vegetable oils. *Lebensmittel-Wissenschaft & Technologie*, Article 116342.
Magzoub, R. A. M., Yassin, A. A. A., Abdel-Rahim, A. M., Gubartallah, E. A., Miskam, M., Saad, B., & Sabar, S. (2019). Photocatalytic detoxification of aflatoxins in Sudanese peanut oil using immobilized titanium dioxide. *Food Control, 95*, 206–214.
Mao, J., He, B., Zhang, L., Li, P., Zhang, Q., Ding, X., & Zhang, W. (2016). A structure identification and toxicity assessment of the degradation products of aflatoxin B1 in peanut oil under UV irradiation. *Toxins, 8*(11), 332.
Marchese, S., Polo, A., Ariano, A., Velotto, S., Costantini, S., & Severino, L. (2018). Aflatoxin B1 and M1: Biological properties and their involvement in cancer development. *Toxins, 10*(6), 214.
Meng, P., Li, J., Wang, P., Yang, G., Liu, W., Liang, S., … Sun, C. (2024). In-situ construction of Z-scheme silver phosphotungstate/polyimide photocatalysts and enhanced visible-light photocatalytic degradation of aflatoxin B1 in vegetable oil. *Chemical Engineering Journal, 483*, Article 149153.
Mohammed, S., Munissi, J. J., & Nyandoro, S. S. (2018). Aflatoxins in sunflower seeds and unrefined sunflower oils from Singida, Tanzania. *Food Additives and Contaminants: Part B, 11*(3), 161–166.
Moradian, M., Faraji, A. R., & Davood, A. (2024). Removal of aflatoxin B1 from contaminated milk and water by nitrogen/carbon-enriched cobalt ferrite-chitosan nanosphere: RSM optimization, kinetic, and thermodynamic perspectives. *International Journal of Biological Macromolecules, 256*, Article 127863.
Nagendran, V., Goveas, L. C., Vinayagam, R., Varadavenkatesan, T., & Selvaraj, R. (2024). Nanozymes in environmental remediation: A bibliometric and comprehensive review of their oxidoreductase-mimicking capabilities. *Microchemical Journal*, Article 111748.
Nazareth, T. D. M., Soriano Pérez, E., Luz, C., Meca, G., & Quiles, J. M. (2024). Comprehensive review of aflatoxin and ochratoxin A dynamics: Emergence, toxicological impact, and advanced control strategies. *Foods, 13*(12), 1920.
Nazhand, A., Durazzo, A., Lucarini, M., Souto, E. B., & Santini, A. (2020). Characteristics, occurrence, detection and detoxification of aflatoxins in foods and feeds. *Foods, 9*(5), 644.
Ouyang, H., Yuan, H., Huang, J., Xian, J., Wang, W., & Fu, Z. (2022). CoN_4-supported Co_2N metal clusters for developing sensitive chemiluminescent immunochromatographic assays. *Analytica Chimica Acta, 1232*, Article 340478.
Panel, E. C., Schrenk, D., Bignami, M., Bodin, L., Chipman, J. K., Del Mazo, J., … Wallace, H. (2020). *Risk assessment of aflatoxins in food*.
Pankaj, S. K., Shi, H., & Keener, K. M. (2018). A review of novel physical and chemical decontamination technologies for aflatoxin in food. *Trends in Food Science & Technology, 71*, 73–83.
Peng, Z., Chen, L., Zhu, Y., Huang, Y., Hu, X., Wu, Q., … Yang, W. (2018). Current major degradation methods for aflatoxins: A review. *Trends in Food Science & Technology, 80*, 155–166.
Peng, Z., Zhang, Y., Ai, Z., Pandiselvam, R., Guo, J., Kothakota, A., & Liu, Y. (2023). Current physical techniques for the degradation of aflatoxins in food and feed: Safety evaluation methods, degradation mechanisms and products. *Comprehensive Reviews in Food Science and Food Safety, 22*(5), 4030–4052.
Pitta, M., & Markaki, P. (2010). Study of aflatoxin B 1 production by Aspergillus parasiticus in bee pollen of Greek origin. *Mycotoxin Research, 26*, 229–234.
Qi, L., Ma, Y., Cai, R., Li, Y., Wang, R., Yue, T., Yuan, Y., Gao, Z., & Wang, Z. (2023). Degradation of aflatoxins in apple juice by pulsed light and the analysis of their degradation products. *Food Control, 148*, Article 109648.
Rasheed, U., Ain, Q. U., Ali, A., & Liu, B. (2024). One stone two birds: Recycling of an agri-waste to synthesize laccase-immobilized hierarchically porous magnetic biochar for efficient degradation of aflatoxin B1 in aqueous solutions and corn oil. *International Journal of Biological Macromolecules*, Article 133115.
Rasheed, U., Ain, Q. U., & Liu, B. (2024). Integration of Fe-MOF-laccase-magnetic biochar: From Rational Designing of a biocatalyst to aflatoxin B1 decontamination of peanut oil. *Chemosphere, 367*, Article 143424.
Rawal, S., Kim, J. E., & Coulombe, J. R. (2010). Aflatoxicosis: Lessons from toxicity and responses to aflatoxin B_1 in poultry. *Agriculture, 5*(3), 742–777.
Ren, Z., Luo, J., & Wan, Y. (2019). Enzyme-like metal–organic frameworks in polymeric membranes for efficient removal of aflatoxin B1. *ACS Applied Materials and Interfaces, 11*(34), 30542–30550.
Robert, A., & Meunier, B. (2022). How to define a nanozyme. *ACS Nano, 16*(5), 6956–6959.
Rotimi, O. A., Rotimi, S. O., Goodrich, J. M., Adelani, I. B., Agbonihale, E., & Talabi, G. (2019). Time-course effects of acute aflatoxin B1 exposure on hepatic mitochondrial lipids and oxidative stress in rats. *Frontiers in Pharmacology, 10*, 467.
Rushing, B. R., & Selim, M. I. (2019). Aflatoxin B1: A review on metabolism, toxicity, occurrence in food, occupational exposure, and detoxification methods. *Food and Chemical Toxicology, 124*, 81–100.
Saha Turna, N., Comstock, S. S., Gangur, V., & Wu, F. (2024). Effects of aflatoxin on the immune system: Evidence from human and mammalian animal research. *Critical Reviews in Food Science and Nutrition, 64*(27), 9955–9973.
Senturk, S., & Karaca, H. (2022). First report on the presence of aflatoxins in fig seed oil and the efficacy of adsorbents in reducing aflatoxin levels in aqueous and oily media. *Toxin Reviews, 41*(3), 817–827.
Shanakhat, H., Sorrentino, A., Raiola, A., Romano, A., Masi, P., & Cavella, S. (2018). Current methods for mycotoxins analysis and innovative strategies for their reduction in cereals: An overview. *Journal of the Science of Food and Agriculture, 98*(11), 4003–4013.
Shi, H. (2016). *Investigation of methods for reducing aflatoxin contamination in distillers grains*. : Doctoral dissertation, Purdue University.
Song, C., Yang, J., Wang, Y., Ding, G., Guo, L., & Qin, J. (2024). Mechanisms and transformed products of aflatoxin B1 degradation under multiple treatments: A review. *Critical Reviews in Food Science and Nutrition, 64*(8), 2263–2275.
Su, Z., Du, T., Liang, X., Wang, X., Zhao, L., Sun, J., … Zhang, W. (2022). Nanozymes for foodborne microbial contaminants detection: Mechanisms, recent advances, and challenges. *Food Control, 141*, Article 109165.
Sun, H., He, Z., Xiong, D., & Long, M. (2023). Mechanisms by which microbial enzymes degrade four mycotoxins and application in animal production: A review. *Animal Nutrition*.
Sun, S., Yang, J., Liu, Y., Xie, Y., & Mwabulili, F. (2023). Porous Graphitic phase carbon nitride/graphene oxide hydrogel microspheres for efficient and recyclable degradation of aflatoxin B1 in peanut oil. *Food Chemistry, 417*, Article 135964.
Sun, S., Zhao, R., Xie, Y., & Liu, Y. (2021). Reduction of aflatoxin B1 by magnetic graphene oxide/TiO_2 nanocomposite and its effect on quality of corn oil. *Food Chemistry, 343*, Article 128521.
Vila-Donat, P., Marín, S., Sanchis, V., & Ramos, A. J. (2018). A review of the mycotoxin adsorbing agents, with an emphasis on their multi-binding capacity, for animal feed decontamination. *Food and Chemical Toxicology, 114*, 246–259.
Wang, H., Li, C., Xin, M., Khoo, H. E., Mo, Z., Zhou, S., … Zheng, J. M. (2020). Ultraviolet-LED irradiation effectively detoxified aflatoxin B1 in groundnut oils. *ScienceAsia, 46*(5).
Wang, H. B., Mo, Z. M., Yuan, G. W., Dai, X. D., Zhou, S. Y., Khoo, H. E., & Li, C. (2023). Degradation of aflatoxin B1 in peanut oil by ultraviolet-LED cold-light irradiation and structure elucidation of the degradation products. *Journal of Oleo Science, 72*(4), 473–480.
Wang, F., Xie, F., Xue, X., Wang, Z., Fan, B., & Ha, Y. (2011). Structure elucidation and toxicity analyses of the radiolytic products of aflatoxin B1 in methanol–water solution. *The Journal of Hazardous Materials, 192*(3), 1192–1202.

Wang, L., Zhang, M., Zhang, M., Sun, Z., Ni, Z., Yin, Y., Wu, D., & Yuan, Q. (2025). Construction of carbon-doped iron-based nanozyme for efficient adsorption and degradation to synergistic removal of aflatoxin B1. *Colloids and Surfaces B: Biointerfaces, 245*, Article 114297.

Wei, J., Wu, X., Wu, C., Hou, F., Wu, L., & Huang, H. (2022). Metal-organic frameworks with peroxidase-like activity for efficient removal of aflatoxin B1. *Food Chemistry, 378*, Article 132037.

Wei, J., Yuan, M., Wang, S., Wang, X., An, N., Lv, G., & Wu, L. (2023). Recent advances in metal organic frameworks for the catalytic degradation of organic pollutants. *Collagen and Leather, 5*(1), 33.

Wu, Y., Cheng, J. H., & Sun, D. W. (2021). Blocking and degradation of aflatoxins by cold plasma treatments: Applications and mechanisms. *Trends in Food Science & Technology, 109*, 647–661.

Xu, H., Sun, J., Wang, H., Zhang, Y., & Sun, X. (2021). Adsorption of aflatoxins and ochratoxins in edible vegetable oils with dopamine-coated magnetic multi-walled carbon nanotubes. *Food Chemistry, 365*, Article 130409.

Xu, C., Ye, S., Cui, X., Zhang, Q., & Liang, Y. (2019). Detoxification of aflatoxin B1 in peanut oil by iodine doped supported TiO_2 Thin film under ultraviolet light irradiation. *Current Nanoscience, 15*(2), 188–196.

Yang, L. X., Liu, Y. P., Miao, H., Dong, B., Yang, N. J., Chang, F. Q., … Sun, J. B. (2011). Determination of aflatoxins in edible oil from markets in Hebei Province of China by liquid chromatography–tandem mass spectrometry. *Food Additives and Contaminants: Part B, 4*(4), 244–247.

Yassin, A. A., & Abdelrahman, N. (2019). Effect of alkali refining on removal of aflatoxins in groundnut oil and quality evaluation. *Gezira J. Eng. Appl. Sci, 14*(1).

Ying, Z., Zhang, T., Li, H., & Liu, X. (2023). Adsorptive removal of aflatoxin B1 from contaminated peanut oil via magnetic porous biochar from soybean dreg. *Food Chemistry, 409*, Article 135321.

Yu, Y., Shi, J., Xie, B., He, Y., Qin, Y., Wang, D., … Sun, Q. (2020). Detoxification of aflatoxin B1 in corn by chlorine dioxide gas. *Food Chemistry, 328*, Article 127121.

Zabeti, N., Keyhanizadeh, A. K., Faraji, A. R., Soltani, M., Saeedi, S., Tehrani, E., & Hekmatian, Z. (2024). Activate hydrogen peroxide for facile and efficient removal of aflatoxin B1 by magnetic Pd-chitosan/rice husk-hercynite biocomposite and its impact on the quality of edible oil. *International Journal of Biological Macromolecules, 254*, Article 127897.

Zhang, X., Jiao, R., Ren, Y., Wang, Y., Li, H., Ou, D., … Ye, Y. (2024). Adsorptive removal of aflatoxin B1 via spore protein from Aspergillus luchuensis YZ-1. *Journal of Hazardous Materials, 476*, Article 135148.

Zhang, Y., Li, M., Liu, Y., Guan, E., & Bian, K. (2021b). Degradation of aflatoxin B1 by water-assisted microwave irradiation: Kinetics, products, and pathways. *Lebensmittel-Wissenschaft & Technologie, 152*, Article 112310.

Zhang, Z. S., Xie, Q. F., & Che, L. M. (2018). Effects of gamma irradiation on aflatoxin B1 levels in soybean and on the properties of soybean and soybean oil. *Applied Radiation and Isotopes, 139*, 224–230.

Zhang, K., & Xu, D. (2019). Application of stable isotope dilution and liquid chromatography tandem mass spectrometry for multi-mycotoxin analysis in edible oils. *Journal of AOAC International, 102*(6), 1651–1656.

Zhao, H., Chen, X., Shen, C., & Qu, B. (2017). Determination of 16 mycotoxins in vegetable oils using a QuEChERS method combined with high-performance liquid chromatography-tandem mass spectrometry. *Food Additives & Contaminants: Part A, 34*(2), 255–264.

Zhou, L., Duan, X., Dai, J., Ma, Y., Yang, Q., & Hou, X. (2024). A covalent-organic framework-based platform for simultaneous smartphone detection and degradation of aflatoxin B1. *Talanta, 278*, Article 126505.

Zhu, M., Wen, X., Zhao, J., Liu, F., Ni, Y., Ma, L., & Li, J. (2016). Effect of industrial chemical refining on the physicochemical properties and the bioactive minor components of peanut oil. *Journal of the American Oil Chemists' Society, 93*(2), 285–294.